

Electronic Thesis and Dissertation Repository

8-29-2014 12:00 AM

Investigation of Sox9 ablation on neuroplasticity and recovery after ischemic stroke

Bethany Robin Lenore Bass
The University of Western Ontario

Supervisor
Dr. Arthur Brown
The University of Western Ontario

Graduate Program in Anatomy and Cell Biology
A thesis submitted in partial fulfillment of the requirements for the degree in Master of Science
© Bethany Robin Lenore Bass 2014

Follow this and additional works at: <https://ir.lib.uwo.ca/etd>



Part of the [Neurosciences Commons](#)

Recommended Citation

Bass, Bethany Robin Lenore, "Investigation of Sox9 ablation on neuroplasticity and recovery after ischemic stroke" (2014). *Electronic Thesis and Dissertation Repository*. 2338.
<https://ir.lib.uwo.ca/etd/2338>

This Dissertation/Thesis is brought to you for free and open access by Scholarship@Western. It has been accepted for inclusion in Electronic Thesis and Dissertation Repository by an authorized administrator of Scholarship@Western. For more information, please contact wlsadmin@uwo.ca.

INVESTIGATION OF SOX9 ABLATION ON NEUROPLASTICITY AND
RECOVERY AFTER ISCHEMIC STROKE

Thesis format: Monograph

by

Bethany Bass

Graduate Program in Anatomy and Cell Biology

A thesis submitted in partial fulfillment
of the requirements for the degree of
Master of Science

The School of Graduate and Postdoctoral Studies
The University of Western Ontario
London, Ontario, Canada

© Bethany Bass 2014

Abstract

Neuroplasticity is a key factor in post-stroke functional recovery. A chief inhibitor of post-stroke neuroplasticity is the expression of chondroitin sulfate proteoglycans (CSPGs). Recent research has shown that the transcription factor SOX9 is responsible for upregulating the expression of CSPGs in the injured central nervous system. Accordingly, CSPG levels are significantly lower in mice with the *Sox9* gene conditionally knocked out. The purpose of this study was to determine how *Sox9* ablation affects neuroplasticity and recovery after stroke. Behavioural test results revealed that *Sox9* KO mice exhibited significantly improved functional recovery after stroke compared to controls. This correlated with increased contralesional corticofugal plasticity in the *Sox9* KO animals, as highlighted by tract tracing studies. An increase in one type of glutamatergic input marker (VGLUT1) was observed at the deafferented red nucleus of the *Sox9* KO mice, but not at the denervated the cervical spinal cord ventral horn. Further investigation into the effects of *Sox9* ablation on post-stroke neuroplasticity would be beneficial to determine the potential of *Sox9* as a therapeutic target.

Keywords

Sox9, stroke, ischemia, middle cerebral artery occlusion, recovery, neuroplasticity, chondroitin sulfate proteoglycans, tract tracing, synaptic markers

Acknowledgements

I am indebted to many colleagues, friends and family members who have offered support and wisdom throughout the completion of this work. First and foremost, I would like to thank my supervisor, Dr. Arthur Brown, for his continuous help and guidance. I would also like to thank the members of my Advisory Committee, Drs. Lynne-Marie Postovit, David Cechetto, and Geoffrey Pickering for all their help and advice throughout the completion of this thesis. I am also eternally grateful to all members of the Brown lab who were always there to go above and beyond the call of duty to help and support me:

I thank Monty for always having an epic story to regale myself and the other Brown lab members with, and for ranting enthusiastically on a widespread number of topics. I am also grateful for our countless videogame discussions, and will forever await the day when “Monty’s Videogame Review Vlog” is a real thing.

I thank Steve for showing me the meaning of true strength and will power – as you browsed online for T-shirts that you wanted every day, and never purchased a single one of them. Also thanks to you, Steve, I now know that it is *not* cool to have your photo taken with celebrities. I will be sure not to make that mistake again.

To Kathy, my MCAO studies mentor, I would like to thank you for all your advice and guidance throughout my time in the lab. I thoroughly enjoyed working with you, and hearing all about the chronicles of Nicholas and Claire, as well as the menagerie of animals that you took care of at home.

I would like to give a big congratulatory shout out to Todd and Nicole for winning “Cutest Brown Lab Couple” every single year. I am grateful for your continuous support throughout the past few years, and for always having great music suggestions for me. Also, congratulations on your beautiful little family.

Finally, I am eternally grateful to my parents, Dean and Debra Bass. The completion of this work is greatly attributed to your unconditional love and support.

Statement of work:

Drs. Kathy Xu and Todd Hyrciw of the Brown lab contributed to the work completed in the following thesis. Dr. Kathy Xu performed the middle cerebral artery occlusion surgeries, as well as the laser doppler flowmetry on the mice. Dr. Todd Hyrciw was responsible for carrying out the BDA injection surgeries on the mice. Dr. Xu also served as a second rater of BDA fiber counts in the tract tracing experiments.

Table of Contents

Abstract	ii
Acknowledgements and Statement of Work	iii
Table of Contents	v
List of Figures	viii
List of Abbreviations	ix

1 Introduction

1.1	Stroke prevalence	1
1.2	Risk factors and causes of ischemic stroke.....	1
1.3	Treatments and outcomes of ischemic stroke.....	3
1.4	Ischemic injury to the central nervous system.....	6
1.5	Neuroplasticity in the post-stroke CNS, and how it relates to recovery.....	8
1.6	Limitations to post-stroke CNS neuroplasticity.....	10
1.7	Augmenting neuroplasticity to enhance recovery from CNS injury: Examples from the literature.....	13
1.8	The role of the transcription factor SOX9 in the post-stroke CNS.....	15
1.9	Preliminary work on <i>Sox9</i> ablation in a mouse model of stroke.....	17
1.10	Background Summary and Rationale.....	18
1.11	Hypothesis.....	19
1.12	Objectives.....	20
1.13	Overview of experimental plan.....	20

2 Materials and Methods

2.1	Animals.....	24
2.2	Tamoxifen administration.....	25
2.3	Induction of focal cerebral ischemia.....	25
2.4	Measurement of local cerebral blood flow using Laser Doppler Flowmetry.....	26
2.5	Behaviour: functional neurological tests.....	26
2.5.1	Corner test.....	26

2.5.2	Cylinder test.....	27
2.5.3	Grip strength test.....	28
2.6	Delivery of biotinylated dextran amines.....	28
2.7	Perfusions.....	29
2.8	Immunohistochemistry and analysis for biotinylated dextran amines.....	32
2.8.1	Immunohistochemistry for biotinylated dextran amines.....	32
2.8.2	Analysis of corticorubral projections.....	32
2.8.3	Analysis of corticospinal projections.....	33
2.9	Immunohistochemistry and analysis for glutamatergic input markers VGLUT1 and VGLUT2 at the level of the ipsilesional red nucleus.....	33
2.9.1	Immunohistochemistry for VGLUT1, VGLUT2, and SMI-32.....	33
2.9.2	Analysis of glutamatergic input markers VGLUT1 and VGLUT2 at the level of the ipsilesional red nucleus.....	34
2.10	Immunohistochemistry and analysis for glutamatergic input marker VGLUT1 at the level of the contralesional cervical spinal cord.....	35
2.10.1	Immunohistochemistry for VGLUT1 and NeuN.....	35
2.10.2	Analysis of glutamatergic input marker VGLUT1 at the level of the contralesional cervical spinal cord.....	35
2.11	Immunohistochemistry and fluorescent microscopy for BDA-labeled fibers at the level of the ipsilesional red nucleus.....	36
2.11.1	Immunohistochemistry for BDA-labeled fibers at the level of the ipsilesional red nucleus.....	36
2.11.2	Microscopy for BDA-labeled fibers at the level of the ipsilesional red nucleus.....	36
2.12	Statistics.....	37
3	Results	
3.1	Effects of <i>Sox9</i> ablation on functional recovery after MCAO.....	38
3.1.1	Corner test: Sensory-motor recovery after MCAO was improved in <i>Sox9</i> knockout mice compared to controls.....	38
3.1.2	Cylinder test: Sensory-motor recovery after MCAO was improved in <i>Sox9</i> knockout mice compared to controls.....	41

3.1.3	Grip strength test: Recovery of paretic forelimb strength after MCAO was improved in <i>Sox9</i> knockout mice compared to controls.....	41
3.2	Effects of <i>Sox9</i> ablation on structural neuroplasticity after MCAO.....	46
3.2.1	<i>Sox9</i> ablation led to increased structural plasticity in the contralesional corticorubral tract after MCAO.....	46
3.2.2	<i>Sox9</i> ablation led to increased structural plasticity in the contralesional corticospinal tract after MCAO.....	52
3.3	Effects of <i>Sox9</i> ablation on putative synaptic plasticity after MCAO.....	55
3.3.1	<i>Sox9</i> ablation led to increased levels of VGLUT1 input markers at the deafferented red nucleus six weeks after MCAO.....	55
3.3.2	<i>Sox9</i> ablation did not lead to increased levels of VGLUT1 input markers at the deafferented red nucleus six weeks after MCAO.....	58
3.3.3	<i>Sox9</i> ablation did not significantly change levels of VGLUT1 input markers at the deafferented cervical spinal cord ventral horn six weeks after MCAO.....	58
4	Discussion	63
4.1	The influence of SOX9 on functional recovery after stroke.....	63
4.2	The influence of SOX9 on neuroplasticity after stroke.....	64
4.2.1	Examination of structural neuroplasticity after stroke.....	65
4.2.2	Examination of synaptic neuroplasticity after stroke: glutamatergic input markers at the denervated red nucleus.....	66
4.2.3	Examination of synaptic neuroplasticity after stroke: glutamatergic input markers at the denervated cervical spinal cord ventral horn.....	69
4.3	Conclusions.....	71
	References	73
	Animal Use Protocol Approval	82
	Curriculum vitae	83

List of Figures

Figure 1:	Cellular mechanism for conditional <i>Sox9</i> knockout schematic.....	22
Figure 2:	Experimental timelines.....	30
Figure 3:	Corner test.....	39
Figure 4:	Cylinder test.....	42
Figure 5:	Grip strength test.....	44
Figure 6:	BDA tract-tracing at the level of the red nucleus.....	48
Figure 7:	Confocal photomicrographs of BDA-labeled fibers at the level of the red nucleus.....	50
Figure 8:	BDA tract-tracing at the level of the cervical spinal cord.....	53
Figure 9:	VGLUT1 levels at the ipsilesional red nucleus.....	56
Figure 10:	VGLUT2 levels at the ipsilesional red nucleus.....	59
Figure 11:	VGLUT1 levels at the conralesional cervical spinal cord.....	61

List of Abbreviations

CNS	central nervous system
ChABC	chondroitinase ABC
Cre-ER	Cre-mutated estrogen receptor
CSPG	chondroitin sulfate proteoglycan
C4ST	chondroitin-4-sulfotransferase
DAPI	4',6-diamidino-2-phenylindole
DNA	deoxyribonucleic acid
ECM	extracellular matrix
MCAO	middle cerebral artery occlusion
PBS	phosphate buffered saline
PFA	paraformaldehyde
PNN	peri-neuronal net
RNA	ribonucleic acid
tPA	tissue plasminogen activator
VGLUT	vesicular glutamate transporter
XT-I	xylosyltransferase-I
XT-II	xylosyltransferase-II

Chapter 1:

Introduction

1.1 Stroke prevalence

A stroke is defined as a sudden loss of brain function due to an interruption in blood supply to the brain. Stroke is a leading cause of death worldwide, second only to ischemic heart disease (WHO 2013). Despite the fact that many risk factors for stroke are modifiable (hypertension, activity level, weight etc.), stroke is the third leading cause of death, and the leading cause of long-term disability in adults in Canada (CSN 2012; StatsCan 2012). There are three main types of stroke: ischemic stroke (lack of blood flow), intracerebral hemorrhage (bleeding within the brain), and atraumatic subarachnoid hemorrhage (rupture of an aneurysm at the base of the brain). All three types of stroke can lead to loss of function, but they differ in the subsets of people they usually affect, as well as their causes, treatments, and outcomes. It is a debilitating condition that not only puts significant strain on the approximately 300,000 individuals living with the effects of a stroke in Canada (as well as their family members), but which also burdens the economy (PHAC 2009). Stroke costs approximately \$3.6 billion per year in Canada in health care expenditures, as well as lost economic output and productivity due to long-term disability and premature mortality (PHAC 2009; PHAC 2011). While it is imperative to continue to place emphasis on stroke prevention, such high rates of disability and death due to stroke indicate that new approaches to treatment must be investigated as well.

1.2 Risk factors and causes of ischemic stroke

Ischemic stroke (which is modeled in this study) is described as the blockage of a vessel that supplies blood to the brain. This results in the deprivation of vital glucose and oxygen to the most metabolically active organ in the body. It is the most common type of

stroke and accounts for about 80% of all cases in Canada, while the rest are hemorrhagic (CSN 2011; Lu 2011). There are both potentially modifiable and non-controllable risk factors for ischemic stroke. The most significant risk factor for stroke is a person's age, which is non-modifiable. After 55 years of age, the risk of stroke doubles every decade for both men and women (Sacco, Benjamin et al. 1997; Gorelick and Ruland 2010). More women than men tend to die of stroke each year despite the rate of stroke being 1.25 times higher in men. This can be attributed to the fact that women tend to live longer than men do (Sacco, Benjamin et al. 1997). Heredity also plays a role in a person's risk for ischemic stroke, as increased incidence of stroke among families has been observed. Reasons for this may include heredity of genetic factors that increase susceptibility for risk factors of stroke itself, or family members' exposure to common predisposing environmental and lifestyle factors. In the same way, some ethnicities are known to experience higher rates of incidence and mortality with ischemic stroke. For example, people of African-American descent are more than twice as likely to die of ischemic stroke than Caucasian people; however, this too may also be due to a combination of inherited factors other than race, and environmental factors (Sacco, Benjamin et al. 1997).

Hypertension is considered the most important modifiable risk factor for ischemic stroke. A number of studies have shown that treating hypertension in patients significantly lowers the incidence of stroke among them; data combined from seventeen treatment trials of hypertension worldwide show a 38% reduction in stroke and a 40% reduction in fatal stroke (Sacco, Benjamin et al. 1997). Certain cardiac diseases are also known to increase the incidence of stroke, with atrial fibrillation (irregular heart rhythm) being the most notable, which occurs in almost half of all patients who experience a cardioembolic stroke. Cigarette smoking is known to double a person's risk of suffering an ischemic stroke. Other modifiable risk factors include living a sedentary lifestyle, obesity, diabetes, and hypercholesterolemia, all of which increase a patient's susceptibility for atherosclerosis (Sacco, Benjamin et al. 1997; Lu 2011). The occurrence of transient ischemic attacks can also serve as a warning sign for a future ischemic stroke (Lu 2011).

Whether they are modifiable or not, these risk factors can contribute to the primary causes of ischemic stroke: embolism, or thrombosis. Systemic hypoperfusion can also cause ischemia in the brain, but is less common, and results from decreased cardiac output or hypovolemia (Rovira, Grive et al. 2005). The model used in this research project aims to emulate the majority of ischemic strokes, caused by embolism or thrombosis. About twenty-five percent of ischemic strokes are due to embolism, which occurs when a cerebral artery is blocked by a clot or debris that travels from a distant site in the body (e.g. *cardioembolic* stroke occurs when a clot from the heart dislodges and travels to the brain). Emboli can come from the heart (as mentioned), arteries, and veins, and often occur with medical conditions that lead to abnormally increased tendencies of blood clotting (e.g. antiphospholipid syndrome, deficiencies of anti-clotting factors, supplemental estrogen use, etc.) (Sacco, Benjamin et al. 1997). Emboli can develop on diseased, damaged or prosthetic valves, and atherosclerotic emboli that cause ischemic stroke commonly come from the aortic arch or extracranial arteries. About fifty percent of ischemic strokes are due to thrombosis, in which a thrombus (blood clot), occludes a cerebral artery (Lu 2011). Large-vessel thrombotic strokes are the most common, and are often due to long-term atherosclerosis followed by a rapid blood clot formation. Less commonly, thrombotic strokes in small arteries occur, leading to lacunar infarctions (Zorowitz R 2004).

1.3 Treatments and outcomes of ischemic stroke

Current treatments for ischemic stroke range from acute (within a few hours of stroke onset) to long-term rehabilitation. Currently, the only FDA and Health Canada-approved drug for ischemic stroke treatment is tPA, or recombinant human tissue plasminogen activator, which is considered the gold standard of acute treatment. Tissue plasminogen activator is the major enzyme involved in the breakdown of blood clots, which catalyzes the conversion of plasminogen to plasmin and is most commonly delivered intravenously. A tPA clinical study by the National Institute of Neurological Disorders and Stroke found that, although there was an increased risk for intracerebral hemorrhage to occur with the delivery of tPA, patients who received it within the correct

window of time experienced a 12% increase in excellent functional outcome and a 4% risk reduction in mortality (NINDS 1995). Unfortunately, only a small percent of ischemic stroke patients (estimated at 3%) receive this drug due to its very narrow time window for safe administration, which is 3-4.5 hours post-onset of stroke (Lansberg, Bluhmki et al. 2009; Armstead WM 2010). People who experience a stroke may not recognize their symptoms as being indicative of a medical emergency (e.g. unilateral numbness or weakness of the face, arm or leg, visual problems, difficulty speaking or understanding speech, dizziness, etc.) and may delay seeking medical attention (Moser, Kimble et al. 2006; Lu 2011). Even upon arrival at a hospital, it is necessary to perform a non-contrast head CT to determine whether symptoms are due to an ischemic or hemorrhagic stroke, or an altogether different neuropathology (e.g. tumour, abscess) (Lu 2011). After this initial 3 - 4.5 hour time point, IV tPA treatment to breakdown blood clots is considered ineffective in reducing the amount of infarcted tissue, and increases the risk for intracerebral hemorrhage to occur (NINDS 1995).

Intra-arterial thrombolytic delivery is another option for treatment, and stretches the treatment time window to about six hours after the onset of ischemic stroke. This method involves inserting a microcatheter into the vasculature and delivering thrombolytics locally to the site of the occlusion. This is usually a 1 to 2 hour process that involves simultaneous angiographic imaging. As such, intra-arterial thrombolytic treatment is a much more complicated process than IV tPA therapy, and requires more medical professionals and equipment on hand than the latter; however, it boasts overall superior recanalization rates of major cerebrovascular occlusions compared to tPA, most significantly with large vessel occlusions. There are current clinical trials investigating the combinatorial treatment of tPA and intra-arterial thrombolytic delivery (Grigoryan and Qureshi 2010).

For a number of reasons, IV delivery of tPA may fail, or a patient may simply be ineligible for thrombolytic therapy because the risk for intracerebral hemorrhage or other complications would be too high. In such cases, there are endovascular surgical treatment options. An endovascular thrombectomy involves threading a flexible wire with helical loops into the thrombus and retrieving it. Endovascular thromboaspiration is

another clot extraction approach that combines aspiration and debulking of the thrombus in an attempt to reduce or eliminate clotting. Finally, angioplasty with stent placement is another endovascular option that is still being assessed. Each treatment approach comes with a unique set of procedural complication risks, such as vessel rupture and distal embolization. Many factors must go into consideration when choosing the best option for each patient (Grigoryan and Qureshi 2010).

Time is very much so of the essence when a stroke occurs. Unfortunately, even receiving emergency medical care may not be enough to prevent ischemic brain damage from occurring, which can lead to disability and even death. In a study outlined by the Canadian Stroke Network (a review of hospital records across Canada between April 1, 2008 to March 31, 2009), the in-hospital mortality rate for patients admitted for ischemic stroke was 14% after 30 days in the hospital (CSN 2011). The mortality rates for stroke have declined over the past few decades; however, this means that survivors are increasingly likely to live with functional and cognitive impairments and disabilities. The disabling aspects of stroke seem to be feared more than possible fatality, as surviving stroke victims have stated that they believe that severe disability would be a worse outcome than death (PHAC 2009). Unfortunately, more than half of all long-term stroke survivors (>6 months) acquire some sort of disability (mild to severe), which contributes to lower quality of life (Sacco, Benjamin et al. 1997; Clarke, Marshall et al. 2002; PHAC 2009).

Beyond drug and surgical therapies for ischemic stroke, rehabilitation has proved to be beneficial for functional recovery. More specifically, physiotherapy is one of the most important disciplines in interdisciplinary stroke rehabilitation. Physiotherapy usually starts within the first few days after the onset of stroke, and often continues into the chronic phase. The main goal of post-stroke physiotherapy is to re-establish the patient's ability to independently perform basic activities of daily living, such as feeding, bathing, dressing, and being mobile (Veerbeek, van Wegen et al. 2014). A number of studies and meta-analyses emphasize that higher intensities and quantities of physical therapy practices after stroke lead to better results in terms of functional recovery (Veerbeek, van Wegen et al. 2014). Although a particular method of physiotherapy has

yet to be determined to be superior to others, constraint-induced movement therapy has shown promising results. This involves restraining the limb unaffected by the stroke and intensively using the affected limb (Johansson 2000).

Repetition is key to motor learning, and echoes the Hebbian learning rule that connections between neurons are strengthened when they are activated simultaneously (e.g. long term potentiation) (Veerbeek, van Wegen et al. 2014). The main concept of post-stroke physiotherapy involves the use of exercise to induce activity-dependent modification of synaptic connections and reorganization of cortical areas (Johansson 2000). Unfortunately, certain factors in the post-stroke central nervous system work against this beneficial neuroplasticity. Even with physiotherapy, it is estimated that only about half of all stroke survivors are able to perform all activities of daily living without relying on assistance from others in the long term (Veerbeek, van Wegen et al. 2014). In summary, the drug-based, surgical, and rehabilitative therapies currently available to treat ischemic stroke patients do not add up to a cure, and different avenues of treatment need to be investigated.

1.4 Ischemic injury to the central nervous system

Due to cortical neurons' high metabolic rates and energy substrate limitations (near-exclusive dependence on glucose), the effects of ischemia in the brain are immediate. Within seconds under ischemic conditions, cortical activity local to the embolus or thrombus ceases as the neurons undergo an energy saving response. Transient plasma membrane hyperpolarization due to excessive K^+ efflux occurs, followed by another dramatic rearrangement of ions across the plasma membrane. This anoxic membrane depolarization causes the brain's normal cell-to cell signaling mechanisms to turn dangerous. The resulting excessive release of neurotransmitters (glutamate in particular) is a major cause of ischemic neuronal death. Massive glutamate release (initially by activated glutamatergic neurons, and later by reverse transport by astrocytes) involves the overstimulation of glutamate receptors. This causes glutamate receptor ion channels to allow an excess of Ca^+ , Na^+ , and water into the cell, which is

particularly damaging for neurons. Excess dopamine release can also contribute to neuronal death. This excitotoxicity encourages the spread of cellular depolarization, the depletion of energy stores, and the progression of cell injury cascades. (Lee, Grabb et al. 2000; Moskowitz, Lo et al. 2010).

This is where the concept of the ischemic core and penumbra comes into play. The ischemic core is defined as the area of the brain surrounding the embolus or thrombus where revival of tissue viability is not possible; the ischemic conditions have caused neuronal death. The ischemic penumbra, on the other hand, is an area surrounding the core where mild to moderate hypoperfusion exists. The neurons of this area cannot maintain their electrical activity to function normally; however, their ion channels are preserved so that the neurons can theoretically revert to normal functionality if blood flow is returned in a timely manner (generally within several hours of onset). Despite the obvious merits of post-ischemic reperfusion achieved by delivery of tPA or natural breakdown of the vessel blockage, it also brings its own brand of tissue damage risk in the form of reactive oxygen species (superoxide, hydroxyl, and nitric oxide radicals, etc.) and increased inflammation (Lee, Grabb et al. 2000).

Reactive oxygen species wreak havoc on the integrity of vital cellular components (such as DNA, lipids, proteins and enzymes, etc.), and further deplete cellular energy stores. The production of reactive oxygen species is also stimulated by other ischemic developments, such as Zn^{+} overload and glutamate toxicity (Lee, Grabb et al. 2000). Inflammation is another consequence of ischemia and reperfusion that can worsen tissue injury. Cytokine production is increased, and the invasion of neutrophils ensues, followed by macrophages and monocytes. This leads to microvascular obstruction as well as the production of toxic mediators by activated inflammatory and glial cells of the CNS. All in all, the excitotoxicity, spreading depression, oxidative stress and inflammation within the ischemic tissue ultimately lead to cell death by apoptosis and necrosis. Despite the creation of reactive oxygen species and increased inflammation, reperfusion is still considered ideal for revival of the penumbra if achieved in time (Lee, Grabb et al. 2000). Functional loss experienced after a stroke depends on the extent of the ischemic damage, and the area in the brain in which it occurs.

1.5 Neuroplasticity in the post-stroke CNS, and how it relates to recovery

Neuronal death translates into loss of sensory and motor function, so central nervous system protection is a primary goal in stroke treatment. Despite the level of the success that acute neuroprotective and rehabilitative treatment strategies have attained, there are still many limitations. As such, another important area of research centers on understanding the endogenous restorative processes of the post-stroke central nervous system, so that we may develop ways to augment and facilitate these processes to improve recovery (Moskowitz, Lo et al. 2010). Recovery after stroke is variable, but most sensory and motor recovery is generally observed within the first six months, (Wade and Hewer 1987; Bonita and Beaglehole 1988; Reding and Potes 1988; Murphy and Corbett 2009). Similar patterns of spontaneous recovery (further augmented by rehabilitative therapy) can be seen in animal models, although the improvements seem to occur over a much shorter period of time than in humans (Murphy and Corbett 2009). Under normal circumstances, motor and sensory cortices are loosely organized into functional maps, which can undergo modifications and plastic changes by experience and use. When stroke causes damage to these regions, it has been shown that the CNS undergoes a more pronounced "re-mapping" as recovery occurs (Murphy and Corbett 2009).

Many correlations between recovery of function and post-stroke neuroplasticity in both the peri-infarct and more distant, unaffected parts of the CNS have been documented in the literature. For example, a number of functional MRI studies have shown that peri-infarct areas are highly active during recovery in both humans and animal models (Dijkhuizen, Singhal et al. 2003; Chopp, Zhang et al. 2007). Other findings in human and animal models describe how partial recovery of hemiparesis (caused by a stroke involving the contralateral primary motor cortex) often involves either the activation of regions in the opposite undamaged hemisphere, or the activation of undamaged neurons ipsilateral to the stroke that are recruited to serve new functions (Pineiro, Pendlebury et al. 2001; Feydy, Carlier et al. 2002; Schaechter, Kraft et al. 2002; Small, Hlustik et al. 2002; Dijkhuizen, Singhal et al. 2003; Fujii and Nakada 2003; Zemke, Heagerty et al. 2003). Indeed, to the extent that recovery occurs, neural function compromised by

ischemic injury seems to be reallocated to parallel pathways or to new alternate pathways by way of *neuroplasticity*: structural changes in surviving neurons leading to the creation of new neural connections, as well as altered electrical patterns in already existing connections (Lee, Kim et al. 2004; Murphy and Corbett 2009; Moskowitz, Lo et al. 2010).

Neurogenesis is another process in the post-stroke CNS that may play a part in recovery. After cerebral ischemia, newborn neurons originating from the subventricular and subgranular zones in adult mammalian brains (which normally migrate to the hippocampal and olfactory areas) travel towards damaged brain tissue (Arvidsson, Collin et al. 2002; Parent, Vexler et al. 2002). However, many of these newborn cells only survive for a few days, and it is unclear if those that survive contribute significantly to post-stroke recovery. Further research is needed to determine whether or not they develop normally, express neurotransmitters, or become part of functional neural networks (Moskowitz, Lo et al. 2010). It is also fitting to discuss angiogenesis along with neurogenesis, as similar mediators and pathways are involved in both phenomena (Moskowitz, Lo et al. 2010). New neuronal networks are only possible if suitable vascular networks can be established to support them. As such, it is likely that CNS recovery after stroke relies on interdependent neurovascular re-modeling and plasticity that are guided by similar mediators and signals (Murphy and Corbett 2009; Snapyan, Lemasson et al. 2009).

In accordance with the theory that new cells may contribute to new circuits, stem cell therapy has been an appealing avenue of stroke research. However, the improved functional outcome after brain ischemia often seen with stem or progenitor cell administration (e.g. intravenous administration of bone marrow stromal cells in rats) is most likely due to the production of trophic factors by these cells instead of differentiation into neuronal cells (Chen, Li et al. 2001; Murphy and Corbett 2009). The trophic factors released enhance axonal sprouting, the elaboration of dendrites and spines, angiogenesis, and other processes that are important for neuroplasticity; so in extension, these studies further prove the benefits of a plastic CNS for post-stroke recovery, and that

it is important to keep all cell types in mind when examining recovery (neural, glial, and vascular) (Murphy and Corbett 2009).

Accordingly, in principle it would be beneficial to supply the damaged CNS with increased amounts of these trophic factors to augment recovery. The administration of nerve growth factor (NGF), fibroblast growth factor (FGF), glial-derived neurotrophic factor (GDNF), and brain-derived neurotrophic factor (BDNF), for instance, to improve post-stroke recovery have been met with variable levels of success in animal models (Semkova and Kriegelstein 1999). Also of interest are proteins that encourage growth related processes, such as growth-associated protein 43 (GAP-43), myristoylated alanine-rich C-kinase substrate (MARCKS), and brain-abundant signal protein 1 (BASP1) (Murphy and Corbett 2009). Unfortunately, many of these growth-promoting molecules factors are relatively large, making transport past the blood-brain-barrier into the damaged CNS challenging. Further research is needed to optimize trophic and/or pharmacologic factor delivery methods (e.g. using smaller peptides, or transnasal delivery to bypass blood-brain-barrier). Another option would be to focus on compounds that can upregulate the production of endogenous trophic factors (Moskowitz, Lo et al. 2010).

The benefits of neuroplasticity and its associations with recovery in the post-stroke central nervous system have been cited thoroughly in the literature; hence, understanding what facilitates and limits this process could open the door to novel treatment approaches.

1.6 Limitations to post-stroke central nervous system neuroplasticity

Opposite to trophic and growth-promoting factors are negative or inhibitory factors, which also play a big part in orchestrating neuroplasticity. These include components of CNS myelin (e.g. Nogo A, MAG, etc.), inhibitory extracellular matrix (ECM) molecules that are often secreted by astrocytes, and receptors mediating growth cone collapse, which are normally developmentally-regulated (Lee, Kim et al. 2004). Perhaps the most salient of the inhibitory factors expressed in the injured CNS is a family

of ECM molecules called chondroitin sulfate proteoglycans (CSPGs) (Eddleston and Mucke 1993; Fawcett and Asher 1999; Silver and Miller 2004). They have been shown to inhibit neurite outgrowth in many *in vitro* and *in vivo* studies. When a sprouting axon's growth cone comes in contact with CSPGs, protein tyrosine phosphate (PTP) receptors are activated, and the resulting signaling pathways lead to growth cone collapse (McKeon, Schreiber et al. 1991; Meiners, Powell et al. 1995; Davies, Fitch et al. 1997; Zuo, Neubauer et al. 1998). CSPGs are composed of one of a variety of core proteins covalently linked to chondroitin sulfate glycosaminoglycan chains, and are part of the normal CNS extracellular matrix.

In addition to serving both structural and functional roles in the generally loosely organized ECM throughout the CNS, CSPGs are also constituents of structures called *peri-neuronal nets*: highly condensed matrix arrangements surrounding the cell bodies and proximal dendrites of certain classes of neurons, which serve to stabilize synapses and limit synaptic plasticity. The importance of peri-neuronal nets is seen especially in the "critical period" of postnatal CNS development. This is a time when the CNS is particularly plastic, in which appropriate experience leads to the organization of proper neuronal networks. A lack of appropriate experiences may cause the formation of incorrect neuronal connections (Wang and Fawcett 2012). The high degree of plasticity and responsiveness to experience-based neuronal network formation in the critical period has been well studied in the visual system. The end of the postnatal critical period is marked by peri-neuronal net (PNN) deposition around neurons, which stabilizes established connections in the CNS and limits plastic changes due to future experiences (Wang and Fawcett 2012). Along with the establishment of peri-neuronal nets, then end of critical period is also marked by a general upregulation of CSPGs in the CNS (Carulli, Pizzorusso et al. 2010). After full CNS development, the disruption of PNNs can reactivate plasticity and allow for activity-dependent changes to more easily modify neuronal circuits (Wang and Fawcett 2012). However, despite their essentiality to the proper development and function of the uninjured CNS, CSPGs can be detrimental to the injured CNS (Galtrey and Fawcett 2007).

The expression of both axonal growth-promoting and growth-inhibiting genes is induced in specific waves and sequences in the post-stroke CNS (Carmichael, Archibeque et al. 2005). The two main CNS regions that naturally experience tissue re-organization (due to ischemic damage and the balance between these positive and negative factors) include a small area of cortex adjacent to the infarct area, as well as a broader region including peri-infarct cortex and more distant CNS areas. As previously discussed, due to reduced blood flow, the area closely bordering the infarct core experiences oxidative DNA and protein damage, cell death, and reactive astrogliosis (increase of astrocyte number and activation) (Katsman, Zheng et al. 2003; Carmichael, Archibeque et al. 2005). A consequence of astrocyte activation in this region is a massive increase in the production of axonal growth-inhibiting CSPGs. Interestingly enough, this region simultaneously experiences increased expression of all of the growth-promoting genes soon after injury as well. Despite this, axonal growth is limited in this area by the negative factors present, which may serve to decrease aberrant connectivity or simply interfere with the recovery process (Murphy and Corbett 2009).

The second area of interest (peri-infarct and more distant regions), however, experiences *reduced* CSPG expression (which translates to diminished peri-neuronal nets), as well as an increase in the expression of growth promoting genes. This combination allows for increased axonal sprouting to occur in these areas, without detrimental astrocyte activation and cell death (Carmichael 2003; Carmichael, Archibeque et al. 2005). Unfortunately, this decrease in CSPG expression is transient. Animal studies have shown that CSPG expression levels in these peri-infarct and remote CNS areas gradually increase over a month's time to return to normal levels, essentially closing the window of time for increased plasticity to occur (Carmichael, Archibeque et al. 2005). Therefore, a possible strategy to improve recovery after stroke could be to lessen growth-inhibiting factors, thereby altering the CNS microenvironment to better promote beneficial neuroplasticity and axonal sprouting.

1.7 Augmenting neuroplasticity to enhance recovery from CNS injury: Examples from the literature

This strategy to improve recovery has been explored in animal models of a number of different CNS injuries, and most commonly in spinal cord injury (SCI). For example, Huang *et al* used myelin immunization in mice to stimulate the creation of polyclonal antibodies to block myelin-associated axonal growth inhibitors. This resulted in increased CNS axonal growth and regeneration in mice after SCI, and corresponding improvements in hind leg function (Huang, McKerracher *et al.* 1999). In a similar fashion, anti-Nogo antibodies, as well as peptide antagonists of Nogo-66 (which bind to the Nogo receptor) have been used to augment axonal growth and the neuroplastic response to improve functional recovery in rodent models of SCI (Schnell and Schwab 1990; Bregman, Kunkel-Bagden *et al.* 1995; Brosamle, Huber *et al.* 2000; GrandPre, Li *et al.* 2002; Li and Strittmatter 2003). Related strategies have been implemented in studies with animal models of stroke. For example, Papadopoulos, Tsai *et al* used an antibody to block the inhibitory protein Nogo-A in rats after middle cerebral artery occlusion (a model of ischemic stroke), and observed increased axonal growth and functional recovery in the treated animals (Papadopoulos, Tsai *et al.* 2002). Lee, Kim *et al* employed genetic (hetero- and homozygous Nogo receptor knockouts) as well as pharmacologic methods to diminish the Nogo-Nogo receptor system in rodents. Using rodent models of stroke, they found in both cases that axonal plasticity and behavioural function were enhanced after stroke when compared to control animals (Lee, Kim *et al.* 2004).

Perhaps most pertinent to this study is research that focuses on decreasing levels of CSPGs in an attempt to improve neuronal plasticity and recovery after CNS injury. One popular technique is to administer Chondroitinase ABC (ChABC): a bacterial enzyme that catalyzes the degradation of CSPGs by cleaving off glycosaminoglycan chains. Besides numerous *in vitro* studies demonstrating ChABC's ability to degrade CSPGs and increase axonal plasticity, many proof of principle *in vivo* studies have been done with ChABC as well (Fidler, Schuette *et al.* 1999; Schmalfeldt, Bandtlow *et al.* 2000). For example, although not a model of a common human CNS injury, treating mice with ChABC at the lesion site after performing a unilateral nigrostriatal axotomy on them was found to improve neuroplasticity. By diminishing inhibitory CSPG

accumulation, the full development of a glial scar was prevented, which allowed axons to extend across the lesion (Li, Homma et al. 2007). As with other strategies to improve neuroplasticity, the use of ChABC has been examined in more complex CNS injuries, like SCI. Bradbury, Moon *et al* treated spinal cord injured rats with intrathecal injections of ChABC at the level of the lesion. This led to the degradation of CSPGs at the injury site, and a consequent increase in neurite growth-associated proteins in injured neurons. Tract tracing experiments also displayed regeneration of both ascending and descending spinal axons. Electrophysiological tests highlighted the restoration of post-synaptic activity below the lesion with ChABC treatment. All findings correlated with improved locomotor and proprioceptive functional recovery in the ChABC treated rats, emphasizing the therapeutic potential of targeting CSPGS in the injured CNS (Bradbury, Moon et al. 2002).

One recent and particularly relevant study involves ChABC treatment in a rat model of stroke (Soleman, Yip et al. 2012). Unlike other investigations of stroke therapies in rodents that often target the lesioned area itself, Soleman *et al* concentrated on more remote CNS areas for ChABC treatment. By administering ChABC into the denervated side of the cervical spinal cord (relevant for forelimb function) 3 days post-stroke, they hoped to induce localized plasticity of the spinal circuitry. Histological analysis of the cervical spinal cord one week after ChABC injection showed unilateral degradation of CSPGs, and reduced peri-neuronal net presence (by use of 2B6 and WFA antibodies, respectively). Histological analysis of anterograde tract-tracing (by injecting BDA into the contralesional motor cortex) in the cervical spinal cord showed an increase in BDA-labeled collaterals sprouting on the deafferented side in ChABC-treated animals. In accordance with increased neuroplasticity, they found that ChABC treatment also significantly improved forelimb motor recovery by use of the staircase and cylinder tests, as well as forelimb sensory recovery with a bilateral tactile stimulation test (Soleman, Yip et al. 2012).

Thus, a number of studies have shown that a decrease in CSPGs creates a CNS environment that encourages neurite-growth, reactivates plasticity, and promotes functional recovery within the CNS after a number of injuries, including stroke.

Although ChABC treatment may seem promising, the actual process of injecting the CNS tissue is challenging and invasive, and treatment is limited to the areas surrounding the injection sites. ChABC also has the major disadvantage of being unable to completely digest the glycosaminoglycan chains from the core protein of CSPGs (Caterson, Christner et al. 1985). This leaves carbohydrate "stubs" behind, which are less inhibitory to neurite growth than the complete chains, but which can still reduce axon regeneration ability (Lemons, Sandy et al. 2003). Therefore it would be beneficial to investigate methods to prevent the increased production of CSPGs after CNS injury.

One such investigation by Grimpe, Silver *et al* used a ribozyme-based strategy to target xylosyltransferase-I (XT-I), an enzyme involved in CSPG production that initiates the synthesis of chondroitin sulfate side chains. By decreasing XT-I messenger RNA, they were able to show a strong reduction in the levels of inhibitory GAG chains in the rodent lesion penumbra after SCI, which led to the regeneration of axons well beyond the core lesion (Grimpe and Silver 2004). However, like with ChABC, the delivery of this ribozyme is also limited to the areas surrounding the injection site. Therefore, it would be beneficial to investigate how decreasing CSPGs in a more global manner in the CNS could affect recovery after CNS injury as well.

1.8 The role of the transcription factor SOX9 in the post-stroke CNS

To target CSPGs on a more global CNS basis, it is important to understand the process of CSPG production. Synthesis of the chondroitin sulfate side chains is initiated by adding xylose to a serine component of the core protein. This is the rate-limiting step in the production of chondroitin sulfate side chains, and is completed by the enzyme xylosyltransferase (XT, as mentioned previously). XT exists in two isoforms that are encoded by two different genes, XT-I and XT-II (Schwartz 1977; Kearns, Campbell et al. 1991; Gotting, Kuhn et al. 2000). Next, these side chains are sulfated by either chondroitin 4-sulfotransferase (C4ST) (Yamauchi, Mita et al. 2000), or chondroitin 6-sulfotransferase (C6ST), (Fukuta, Uchimura et al. 1995). However, C4ST is the main type present in astrocytes (Gallo and Bertolotto 1990). Our lab has identified the

transcription factor SOX9 as being responsible for upregulating the expression of XT-I, XT-II, and C4ST with bioinformatics and in vitro studies (Gris, Tighe et al. 2007). Unpublished chromatin immunoprecipitation experimental data confirms that the regulation is likely direct. This discovery led our lab to develop the hypothesis that SOX9 inhibition after a CNS injury would lead to decreased CSPG production, and consequently, a microenvironment that better promotes nerve growth and neurological recovery.

Sox9 is part of a family of transcription factors composed of 20 different genes, all with a high mobility group (HMG-box) DNA binding domain of similar sequence homology to that of the Y chromosome-encoded testis determining factor SRY (Moniot, Declosmenil et al. 2009). *Sox9* plays a critical role in sex determination, and in nervous system development. Since conventional *Sox9* knockout mice do not survive perinatally (Bi, Huang et al. 2001), it was necessary to use a conditional *Sox9* knockout line of mice to study the role of SOX9 in recovery from CNS injury (Outlined in 2.1 of Methods and Materials).

We have studied the role of SOX9 after spinal cord injury for several years now by crossing mice obtained from Dr. Andreas Schedl (mice with floxed *Sox9* alleles) with mice obtained from Jackson Laboratories (mice with Cre-recombinase fused to the mutated ligand binding domain of the human estrogen receptor). The resulting mouse line containing both floxed *Sox9* and Cre recombinase allowed us to examine the molecular, cellular, and neurological responses to spinal cord injury in which SOX9 expression levels were reduced in all cell types. It was confirmed that these mice did, in fact, exhibit significantly lower levels of *Sox9* mRNA and protein with real-time PCR and western blot analyses (McKillop, Dragan et al. 2013). After inducing a 70 kdyne contusion spinal cord injury in the mice, *Sox9* knockout mice experienced improved recovery in hind limb function as measured by the Basso mouse scale (BMS), which examines ankle movement and walking ability. Using rodent activity boxes, it was found that *Sox9* knockout mice locomoted to a greater extent than the control mice after injury. Improvements in functional recovery were associated with reduced astrocytic activation as well as lower CSPG levels at the lesion site in *Sox9* knockout animals compared to

control animals (McKillop, Dragan et al. 2013). Success with improving function after SCI in mice led us to consider applying *Sox9* ablation in other models of CNS injury. Hence, similar studies to examine the effects of *Sox9* ablation in a mouse model of stroke were carried out.

1.9 Preliminary work on *Sox9* ablation in a mouse model of stroke

Prior to this study, Dr. Kathy Xu of the Brown lab had done preliminary work characterizing the effects of conditional *Sox9* ablation in a mouse model of stroke. Since ischemic stroke in human patients usually results from a thrombotic or embolic occlusion in a major cerebral artery, and most often the middle cerebral artery (MCA), a commonly used method to reproduce stroke in animals is to occlude temporarily the MCA (Durukan and Tatlisumak 2007; Liu and McCullough 2011). As such, MCAO (middle cerebral artery occlusion) is the stroke model used in this study. The following preliminary findings are currently unpublished. To begin, all animals underwent surgical intra-arterial suture occlusion of the middle cerebral artery through the internal carotid artery. The suture was removed 30 minutes later, which allowed reperfusion of the affected area. This injury model causes rapid infarction of the striatum, and delayed infarction in the overlying cortex (Carmichael 2005). Longer occlusion times can lead to widespread malignant infarction in the rodent brain, which does not model the most common cases of human stroke (Carmichael 2005).

To ensure that the size and area of the infarcts produced after MCAO were equal among *Sox9* knockout and control animals, 2,3,5-triphenyltetrazolium chloride (TTC) staining was performed on the animals' brains 24 hours after injury. The infarct volumes were found to be statistically equivalent between groups, indicating that equal injuries were being produced after the 30 minute MCAO. After ensuring an equal injury, histological, western blot, and densitometric analyses confirmed that SOX9 protein levels were significantly reduced in the brains of the *Sox9* KO animals when compared to controls two weeks after MCAO (more pronounced on the side of the brain ipsilateral to injury). Next, it was logical to examine if this reduction in SOX9 affected CSPG levels

in the injured central nervous systems of both sets of mice. CSPG levels of the diffuse ECM, as well as levels of the CSPG-rich highly condensed matrix structures called perineuronal nets were examined two weeks after MCAO (using CS56, and WFA antibodies, respectively). Histological, western blot and densitometric analyses of CS56 two weeks post-MCAO showed a significant reduction of diffuse extra-cellular matrix CSPGs in the striata of *Sox9* KO mice compared to controls (again, even more profoundly on the side ipsilateral to injury).

Levels of synapse-stabilizing PNNs were examined at more remote CNS areas that are particularly relevant to motor function in the mouse: the red nucleus (a midbrain neuronal cluster that plays an important role in locomotion and skilled limb movements) (Muir and Whishaw 2000), and the ventral horn of the cervical spinal cord (where motor neurons controlling forelimb functions receive input from the brain) (Lemon 2008). In both cases, histological and immunoreactivity imaging analyses confirmed that PNN levels (examined with wisteria floribunda agglutinin or WFA) were significantly lower on the deafferented sides of both the red nucleus and cervical spinal cord of the *Sox9* knockout mice compared to controls two weeks after MCAO. Altogether, these data show that our tamoxifen-inducible conditional *Sox9* knockout model works as hypothesized, in that SOX9 and CSPG levels are significantly reduced in the CNS after stroke. This study focuses on answering important follow-up questions to these preliminary finding: How does the ablation of *Sox9* and the consequent reduction in CSPG and PNN levels in the CNS affect neuroplasticity and functional recovery after stroke?

1.10 Background Summary and Rationale

Ischemic stroke is a detrimental vascular occurrence in which blood flow to the brain is interrupted. It is a leading cause of death and disability worldwide, and requires further investigation into better avenues for treatment. Recovery can occur after a stroke, but is often limited, and will plateau after about 6 months. Any recovery that does occur is generally attributed to neuroplasticity: the central nervous system's ability to

reconfigure in an attempt to take over for lost and damaged functions. Something that limits this post-stroke neuroplasticity is the expression of extracellular matrix molecules called chondroitin sulfate proteoglycans (CSPGs). CSPGs can act as physical and molecular barriers to neuronal growth, and are also a component of highly condensed matrix structures called peri-neuronal nets, which stabilize synapses and limits neuroplasticity. Our research group has identified the transcription factor SOX9 as responsible for upregulating the expression of CSPGs in the injured brain. We hypothesized that by conditionally knocking out the gene *Sox9* in mice, the expression of CSPGs would decrease. This would create a CNS microenvironment that is more conducive to neuroplastic events, and in turn, lead to increased neurological recovery after stroke.

To summarize:

- Normal recovery after stroke, however limited, is generally due to neuroplasticity.
- CSPGs, the expression of which is upregulated after a CNS injury like stroke, inhibit neuroplasticity.
- Work done in our lab has shown that SOX9 is a transcription factor that increases CSPG expression in the injured CNS. By conditionally knocking out *Sox9*, we can decrease CSPG and peri-neuronal net levels in the mouse CNS.
- The purpose of this study is to investigate if a decrease in SOX9 and consequently CSPG expression will lead to increased neuroplasticity, and in turn, improved functional recovery after stroke.

1.11 Hypothesis

I hypothesize that conditional ablation of *Sox9* in mice will lead to increased functional recovery after middle cerebral artery occlusion (a rodent model of stroke), and will be accompanied by increased neuroplasticity when compared to control mice.

1.12 Objectives

The objectives of this study are to:

- 1) Investigate the effects of conditional *Sox9* ablation in mice on neurological and functional recovery after MCAO compared to control mice (by use of corner, cylinder, and grip strength tests).
- 2) Evaluate neuroplasticity after MCAO in mice, and compare between *Sox9*-ablated animals and controls (by use of corticorubral and corticospinal tract tracing, as well as immunohistological examination of synaptic marker expression levels).

1.13 Overview of experimental plan

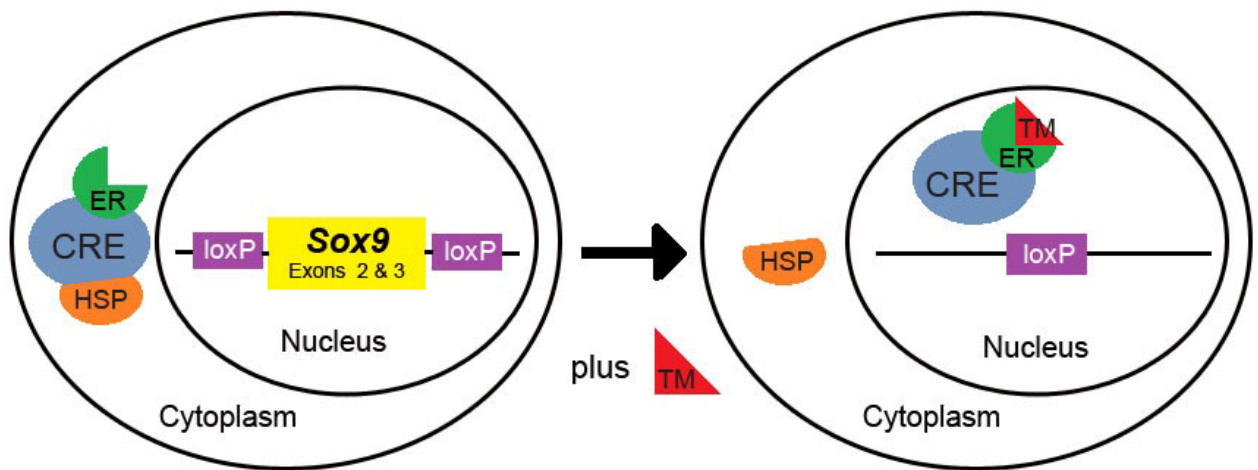
Objectives 1 and 2 are approached using the same experimental timeline. Using a Cre-loxP strategy, both *Sox9^{fllox/fllox};Cre* and *Sox9^{fllox/fllox}* mice are administered tamoxifen to induce *Sox9* ablation in the *Sox9^{fllox/fllox};Cre* mice. This Cre-LoxP strategy is outlined in Figure 1. After tamoxifen administration, a one-week washout period occurs to allow recombination to occur, and for tamoxifen to leave the system. During this week, pre-injury behavioural test data are acquired. Thereafter, both sets of mice undergo left-sided MCAO surgery. A small number of animals of both genotypes are subjected to sham surgeries, to serve as another type of control. Data for Objective 1 are obtained by doing behavioural testing with the mice (corner, cylinder, and grip strength tests) for the subsequent 4 weeks, and comparing results between *Sox9*-ablated animals and controls. Next, a tract tracing experiment begins in the same animals by injecting BDA into the right (unaffected) motor cortex. Two weeks later, the animals are perfused and the brain and spinal cord tissues are sectioned to use for histological analysis.

For Objective 2, neuroplasticity is evaluated at two areas of the central nervous system that are important for the motor functions analyzed in the behavioural tests: the red nucleus within the brain, and the cervical enlargement of the spinal cord. To evaluate structural neuroplasticity, BDA is injected into the right motor cortex (uninjured side)

and BDA-labeled fibers on both sides of the red nucleus and cervical spinal cord are counted. The number of BDA-labeled fibers on the deafferented side of each CNS location is normalized to the number of fibers on the opposite side (to control for labeling efficiency), and results are compared between *Sox9*-ablated and control animals. To examine putative synaptic neuroplasticity, immunohistochemistry is used to stain for glutamatergic synaptic markers (vesicular glutamate transporter 1 and 2, or VGLUT1 and VGLUT2). On the deafferented side of each area (left-sided red nucleus and right-sided cervical spinal cord), signal over background levels of VGLUT staining is calculated, (as area/area or volume/volume) and compared between *Sox9*-ablated and control animals. Results for sham animals are also assessed. To add a more acute post-injury time point to the red nucleus VGLUT1 and VGLUT2 data, brain sections from a previous experiment in which both *Sox9^{flox/flox};Cre* and *Sox9^{flox/flox}* animals were perfused 48 hours after MCAO are also used.

Figure 1: A schematic representation of the Cre-loxP strategy to knockout the *Sox9* gene. In *Sox9^{fllox/fllox}*;Cre mice, the administration of tamoxifen (TM) releases heat-shock protein 90 from the Cre-ER protein complex, allowing it to enter the nucleus of the cell. Exons 2 and 3 of the *Sox9* gene between the loxP sites are excised, effectively preventing SOX9 expression. Tamoxifen is also administered to the *Sox9^{fllox/fllox}* mice; however, there is no Cre-ER present within the cells to excise the *Sox9* gene, so SOX9 expression is normal.

Cellular mechanism for conditional *Sox9* knockout



Chapter 2:

Materials and Methods

2.1 Animals

Conventional *Sox9* knockout mouse embryos (homozygous and heterozygous, *Sox9*^{-/-} and *Sox9*^{+/-}, respectively) are not viable (Bi, Huang et al. 2001). As such, a tamoxifen-inducible conditional *Sox9* knockout strategy was used to allow the mice to progress through development with normal SOX9 activity. We bred a mouse strain (obtained from Dr. Andreas Schedl) carrying floxed *Sox9* alleles (exons 2 and 3 of *Sox9* surrounded by loxP sites) (Akiyama, Chaboissier et al. 2002) with a transgenic mouse line ubiquitously expressing Cre recombinase fused to the mutated ligand binding domain of the human estrogen receptor (ER) under the control of a chimeric cytomeglovirus (CMV) immediate-early enhancer/chicken β-actin promoter (B6.Cg-Tg(CAG-Cre / *Esr1*)5*Amc* / J) (Jackson Laboratories, Bar Harbor, ME). The two populations of resulting offspring served as tamoxifen-inducible *Sox9* knockout mice (*Sox9*^{flox/flox}; CAGGCreER, here after referred to as *Sox9*^{flox/flox}; Cre), and control mice with normal expression levels of *Sox9* (*Sox9*^{flox/flox}). Polymerase chain reaction analysis was used to genotype the animals using the following primers:

Sox9^{flox} allele: 5'-ACACAGCATAGGCTACCTG-3' and
5'-GGTAATGAGTCATACACAGTAC-3'.

Sox9^{wildtype} allele: 5' GGGGCTTGTCTCCTTCAGAG-3' and
5'-TGGTAATGAGTCATACACAGTAC-3'.

Sox9^{knock-out} allele: 5'-GTCAAGCGACCCATG-3' and
5'-TGGTAATGAGTCATACACAGTAC-3'.

Cre⁺ allele: 5'-CAATTTACTGACCGTACAC-3' and
5'-AGCTGGCCCAAATGTTGCTG-3'.

2.2 Tamoxifen administration

Both *Sox9^{flox/flox};Cre* and *Sox9^{flox/flox}* mice were administered tamoxifen (Sigma Aldrich, St. Louis, MO) by oral gavage at a dose of 3 mg/20 g mouse. The drug was given once a day for 7 days, followed by a 7 day period without treatment (to allow for Cre-mediated recombination and tamoxifen clearance to occur before MCAO surgery).

2.3 Induction of focal cerebral ischemia

All protocols for these experiments were approved by the University of Western Ontario Animal Care Committee in accordance with the policies established in the Guide to Care and Use of Experimental Animals prepared by the Canadian Council on Animal Care. Male mice weighing 25-30g were allowed free access to food and water. One week after the last dose of tamoxifen was administered, mice were anesthetized with 4% isoflurane and maintained at 1.5% isoflurane and 30% O₂. Body temperature was maintained using a heating pad. Cerebral ischemia was induced using an intraluminal filament technique (protocol outlined by (Rupadevi, Parasuraman et al. 2011)). A midline neck incision was made and left common and external carotid arteries were isolated and ligated. A 5-0 nylon monofilament coated with 0.1% poly-L-lysine was introduced through a small incision into the common carotid artery and advanced to the carotid bifurcation for middle cerebral artery occlusion (MCAO). Reperfusion was initiated 30 minutes later by monofilament withdrawal. The mortality rate for these mice was approximately 15%. In sham-operated animals, the monofilament was placed into the MCA and withdrawn immediately. Animals were administered Baytril (25 mg/kg, Bayer, Toronto, Ontario, Canada) and buprenorphine (0.01 mg/kg, Schering-Plough, Hertfordshire, UK) subcutaneously after MCAO, and then twice daily for three days after the surgery. If mice showed no signs of functional deficits (circling, etc.) after the 30 minute MCAO, they were not included in the study.

2.4 Measurement of local cerebral blood flow using Laser Doppler Flowmetry

Laser Doppler Flowmetry was used to measure cerebral blood flow and verify that MCAO had occurred. This test was done on a separate set of animals to ensure the reproducibility of the MCAO (n=3). The OXYLAB flowmeter is equipped with a small-caliber probe of 0.7mm diameter (Oxford Optronix, Oxford, UK). The mice were placed in a stereotaxic frame with a mouse holder, and anesthetized with 4% isoflurane and maintained at 1.5% isoflurane and 30% O₂. Body temperature was monitored and maintained using a heating pad. A midline incision was made and a burr-hole (0.7 mm in diameter) was drilled 1mm posterior and 4mm lateral to the sagittal suture on the left side of the skull. The probe was held in a micromanipulator and was stereotaxically advanced to gently touch the dura covering the ischemic core region. Warm saline (37°C) was slowly rinsed around the probe and maintained a clear medium between the probe and the dura during the measurement. Stable baseline laser doppler flowmetry readings were obtained prior to MCAO surgery. The changes of regional CBF were recorded 5 minutes into the occlusion of the middle cerebral artery. A sharp drop over 85% (85.8±2.5%) of baseline was noted, which remained stable throughout the 30 minute occlusion.

2.5 Behaviour: functional neurological tests

2.5.1 Corner test

Initially designed by Schallert *et al* (1982) for rats and later adapted by Zhang *et al* (2002) to mice, the corner test is used to detect sensori-motor and postural asymmetries. The apparatus consists of a corner made by two vertical boards (30 × 20 × 1 cm³) attached on one side with an angle of 30°. A small opening between the boards encourages the mouse to go into the corner. Each mouse is placed at the entry of the corner facing into it. When the mouse reaches the wedge of the corner, both sides of the body (vibrissae, skin) are stimulated simultaneously. Then, the mouse typically rears, and turns either to the right or to the left to exit the corner. Corner tests were carried out before injury, as well as 2 days afterward, and once per week for four weeks

following MCAO surgery. During each test, the mice were tested ten times (about 2 minutes per animal), and the chosen sides were noted. In case of ventral turning (i.e. when the mouse turned without rearing), the trial was not taken into account but repeated at the end of the session.

2.5.2 Cylinder test

The cylinder test was initially used in rats and later adapted for use in mice to assess forelimb use asymmetry (Schallert, Fleming et al. 2000; Li, Blizzard et al. 2004). The mice are placed in a transparent cylinder (9 cm in diameter and 15 cm in height) and videotaped during the test. A mirror is placed behind the cylinder with an angle to enable the observer to record forelimb movements when the mouse is turned away from the camera. After the mouse is put into the cylinder, forelimb use of the first contact against the wall after rearing, and during lateral exploration, is recorded by the following criteria: (1) The first forelimb to contact the wall during a full rear is recorded as an independent wall placement for that limb. (2) Simultaneous use of both the left and right forelimb by contacting the wall of the cylinder during a full rear and for lateral movements along the wall is recorded as a “both” movement. (3) After the first forelimb (for example right forelimb) contacts the wall and then the other forelimb is placed on the wall, but the right forelimb is not removed from the wall, a “right forelimb independent” movement and a “both” movement are recorded. A minimum of 20 movements are recorded during the three minute test. If the mouse did not complete 20 forelimb placements, a second trial was performed later that day. If 20 forelimb placements could not be recorded again, the animal was not included in the study.

Cylinder tests occurred three days after injury, as well as once a week for four weeks following MCAO surgery. The asymmetry score for each test day is calculated as: $(\text{non-impaired forelimb movement} - \text{impaired forelimb movement}) / (\text{non-impaired forelimb movement} + \text{impaired forelimb movement} + \text{both movement})$ as previously described in the rat (Schallert, Fleming et al. 2000). This test evaluates forelimb use asymmetry for weight shifting during vertical exploration and provides high inter-rater

reliability, even with inexperienced raters. Occasionally, mice with large deficits did not move frequently enough to obtain an adequate number of vertical movements.

2.5.3 Grip strength test

The grip strength test was performed using a Grip Strength Meter (Columbus Instrument, Columbus, OH). It employs a triangular steel wire that the animal instinctively grasps. When pulled by the tail, the animal exerts force on the steel wire (Kilic, ElAli et al. 2010). The left forepaw is wrapped with adhesive tape so that grip strength in the right forepaw (affected by the left-sided MCAO) could be evaluated. Grip strength was measured five times in each test, and the highest score was recorded. Grip strength was measured before the MCAO surgery, and then once a week afterwards for four weeks. From these data, percentage values for each week post-MCAO measurement compared to the initial pre-MCAO recording were calculated. If mice consistently failed to grab the steel wire for the proper acquisition of a grip-strength reading, they were not included in the study.

2.6 Delivery of biotinylated dextran amines (BDA)

The protocol for anterograde axonal tract tracing in rats had been established previously (O'Neill and Clemens 2001). Here, we adopted this method to mice. Four weeks after MCAO, the mice were placed in a stereotaxic frame with a mouse holder, and anesthetized with 4% isoflurane and maintained at 1.5% isoflurane and 30% O₂. Body temperature was monitored and maintained at 36°C using a heating pad and rectal thermometer. A small piece of skull (1.5mm in diameter) overlaying the right motor cortex was removed. A total volume of 1.6µl 10% BDA (10,000 MW, Molecular Probes) was administered to each animal, using a Hamilton microsyringe, paired with a 33G needle. Four equal injections were administered to cover the forelimb representation area in the motor cortex, contralateral to the stroke, located at 0.5mm anterior and posterior to the bregma; 1.5mm and 2.5mm lateral to the sagittal suture, respectively, at a depth of

0.5mm. The needle was kept in place after injection for at least 2 minutes to avoid the leakage from the injection site. After all four injections, the incision was sutured. Animals were administered Baytril (25 mg/kg, Bayer, Toronto, Ontario, Canada) and buprenorphine (0.01 mg/kg, Schering-Plough, Hertfordshire, UK) subcutaneously after the surgery, and then twice daily for three days.

2.7 Perfusions

Three weeks post-BDA injection, the mice were deeply anesthetized with 100 mg/kg ketamine: 5 mg/kg xylazine, and transcardially perfused with ice cold saline solution, followed by 4% paraformaldehyde (4% PFA in 0.1 M phosphate buffer at pH 7.4). The experimental timeline is shown in Figure 2. Brains and spinal cords were dissected, post-fixed in 4% PFA for 1 hour, and then cryoprotected in 20% sucrose at 4°C overnight. Brains and spinal cords were dissected and embedded in Tissue Tek O.C.T. Compound (Sakura Finetek USA Inc., Torrance, CA), frozen over dry ice and stored at -80°C. The brains were cross sectioned at 10µm using a cryostat, and serially thaw-mounted on Superfrost™ glass slides (Fisher Scientific Company, Ottawa, Canada). Collected brain sections alternated on 10 slides with 5 sections per slide so each section per slide was separated by 100µm. Cervical spinal cords were cross sectioned at 10µm using a cryostat, and serially thaw-mounted on Superfrost™ glass slides (Fisher Scientific Company, Ottawa, Canada) as well. Collected cervical spinal cord transverse sections alternated on 10 slides with 10 sections per slide so that each section per slide was separated by 100µm.

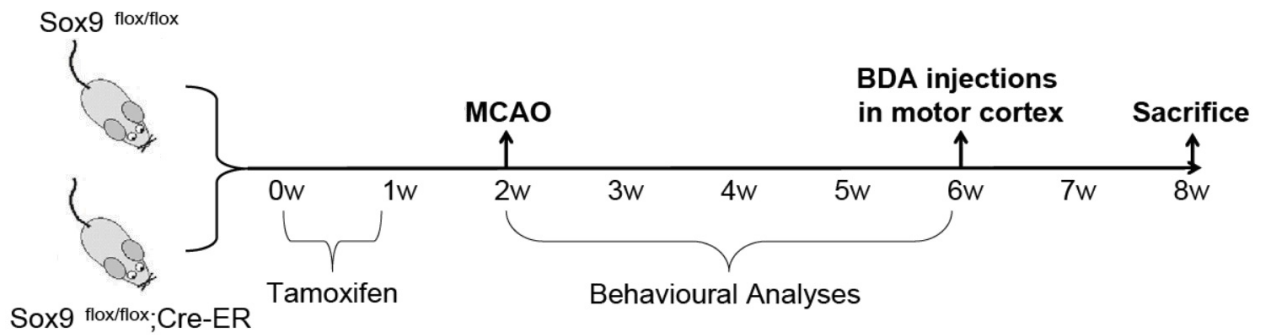
To add a more acute post-injury time point to the red nucleus glutamatergic input data (VGLUT1 and VGLUT2, as described in section 2.9) brain sections from *Sox9^{flox/flox};Cre* and *Sox9^{flox/flox}* animals that were perfused 48 hours after MCAO were also used. The experimental timeline for these animals is also shown in Figure 2. Brains were dissected, sectioned and serially thaw-mounted in the manner described above.

Figure 2: Experimental timelines for both experiments discussed in this thesis

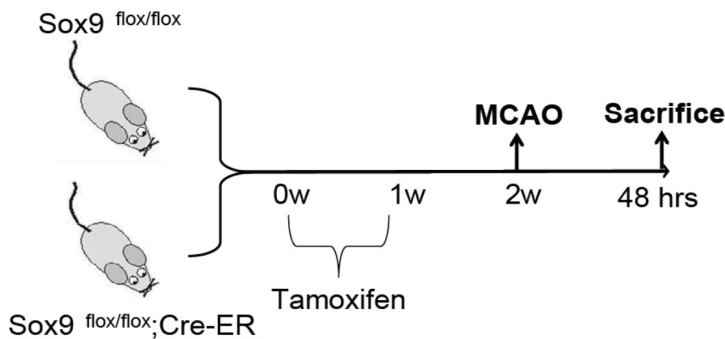
A) Timeline for the MCAO experiment, with behavioural analyses and an anterograde neuronal tracer injection into the contralesional motor cortex. The two groups of mice used include the ubiquitous *Sox9* knockout mice (*Sox9*^{flox/flox};Cre-ER) and their littermate controls (*Sox9*^{flox/flox}).

B) Timeline for the MCAO experiment in which both the ubiquitous *Sox9* knockout mice (*Sox9*^{flox/flox};Cre-ER) and their littermate controls (*Sox9*^{flox/flox}) were sacrificed 48 hours after MCAO. The brain tissue was used to contribute to the VGLUT quantification data.

A Timeline for MCAO experiment, including behavioural analyses and BDA injection in control and *Sox9* knockout mice



B Timeline for past MCAO experiment with 48 hour post-surgery sacrifice in control and *Sox9* knockout mice



2.8 Immunohistochemistry and analysis for biotinylated dextran amines

2.8.1 Immunohistochemistry for biotinylated dextran amines (BDA)

Brain and cervical spinal cord sections were washed three times for 10 minutes in TBS, and then incubated with 0.3% hydrogen peroxide in methanol for 30 minutes to quench the endogenous peroxidase activity. After three more TBS washes, the sections were incubated in blocking solution (5% milk, 1% bovine serum albumin, and 0.3% Triton X-100 in TBS) for 1 hour. Another set of TBS washes followed, and then the sections were incubated with avidin-biotin-peroxidase complex (ABC Elite; Vector Laboratories, Burlingame, CA, USA) in TBS with 0.5% Triton X-100 for 2 hours. After a final set of TBS washes, staining was revealed with a 3,3'-diaminobenzidine reaction (DAB, Invitrogen, Carlsbad, CA). Sections were then washed in dH₂O, dehydrated, and protected with a coverslip using XYL mounting medium (Fisher Scientific Company, Ottawa, Canada).

2.8.2 Analysis of corticorubral projections

Three coronal sections at the level of the parvocellular red nucleus (at least 100 μm apart) were examined to evaluate the corticorubral projections. Images of each section were captured with a 10X and a 20X objective lens (Olympus BX50). First, the labeled fibers from all three sections in the contralesional hemisphere (ipsilateral to BDA injection) projecting to the red nucleus were counted. For each section, the fibers present on the ipsilesional side (contralateral to BDA injection) were quantified and normalized to the total number of the labeled fibers on the contralesional side (to control for labeling efficiency). Fiber numbers were quantified by two separate raters (myself and Dr. Kathy Xu), and then averaged to obtain the final fiber counts. Fibers had to have a minimum length of 3 μm to be counted. Only the animals that had more than 100 labeled fibers on the contralesional side using the 10X objective were included to ensure adequate labeling efficiency.

2.8.3 Analysis of corticospinal projections

Eight transverse spinal cord sections at the level of cervical enlargement (at least 100 μm apart) were examined to evaluate the corticospinal projections. Images of each section were captured with a 10X and a 20X objective lens (Olympus BX50). To begin, in all eight cervical spinal cord sections, the labeled fibers in the grey matter on the contralesional side (ipsilateral to BDA injection) were counted. For each section, the fibers present within the grey matter of the contralesional side of the cervical spinal cord (ipsilateral to BDA injection) were quantified and normalized to the total number of the labeled fibers on the ipsilesional side (to control for labeling efficiency). Fiber numbers were quantified by two separate raters (myself and Dr. Kathy Xu), and then averaged to obtain the final fiber counts. Fibers had to have a minimum length of 3 μm to be counted. Only the animals that had more than 100 labeled fibers on the ipsilesional side using the 10X objective were included to ensure adequate labeling efficiency.

2.9 Immunohistochemistry and analysis for glutamatergic input markers VGLUT1 and VGLUT2 at the level of the ipsilesional red nucleus

2.9.1 Immunohistochemistry for VGLUT1, VGLUT2 and SMI-32

SMI-32 is an antibody for a non-phosphorylated epitope in neurofilament heavy polypeptide, which is found within the neuronal cell bodies, dendrites, and some thick axons of rubrospinal cells in the red nucleus (Liang, Paxinos et al. 2012). This antibody was used to identify the location of the red nucleus. VGLUT1 and VGLUT2 antibodies were used to stain for vesicular glutamate transporter 1, and 2, respectively (markers of glutamate transporters in the membranes of synaptic vesicles). VGLUT1 is the major glutamate transporter expressed in layer V motor cortex neurons (including corticorubral), while VGLUT2 is the major glutamate transporter in cerebellar and thalamic projections to the red nucleus (Allen Brain Atlas - VGlut2 in mouse brain; Allen Brain Atlas - VGlut1 in mouse brain; Naus, Flumerfelt et al. 1986; Roger and Cadusseau 1987; Arnault, Ebrahimi-Gaillard et al. 1994; Varoqui, Schafer et al. 2002; Fink, Englund et al. 2006; Barroso-Chinea, Castle et al. 2007).

Brain sections from Sox9^{fllox/fllox};Cre and Sox9^{fllox/fllox} mice were incubated with blocking solution (5% goat serum in PBS, with 0.1% Triton X-100) at room temperature for 2 hours, and then incubated with primary antibodies diluted in blocking solution at 4°C overnight. The primary antibodies used were: mouse anti-SMI-32 (1:1000, Covance, catalogue # SMI-32R), along with either rabbit anti-VGLUT1 (1:500, Synaptic Systems, catalogue # 135 302) or rabbit anti-VGLUT2 (1:500, Synaptic Systems, catalogue # 135 402). Sections were washed three times for 10 minutes, after which immunofluorescent labeling was performed using the following secondary antibodies (for one hour at room temperature): Alexa Fluor 488 goat anti-mouse IgG (1:500, Life Technologies, catalogue # A-11029), and Alexa Fluor 647 goat anti-rabbit (1:1000, Life Technologies, catalogue # A-21244). After washing three times in PBS for at least 30 minutes, the sections were protected with a coverslip using ProLong Gold Anti-Fade mounting medium with DAPI (Life Technologies, catalogue # P36935).

2.9.2 Analysis of glutamatergic input markers VGLUT1 and VGLUT2 at the level of the ipsilesional red nucleus

Three coronal sections at the level of the parvocellular red nucleus (at least 100 µm apart) were examined to evaluate levels of presynaptic glutamatergic markers within the ipsilesional red nucleus (three sections each for both VGLUT1 and VGLUT2). Z-stacks 2 µm in thickness (composed of 10 sections at a thickness of 0.2µm) were captured with a 40X objective lens with a spinning disk confocal microscope and Volocity software (CSU10, with an Olympus IXS1). Images were deconvoluted with Autoquant X software (Media Cybernetics Inc., Rockville, MD, USA). Using Imaris software (Bitplane AG, Zurich, Switzerland) VGLUT1 and VGLUT2 signal greater than background within the red nucleus was identified and quantified (as volume of immunoreactivity/volume of red nucleus section). Average VGLUT1 and VGLUT2 immunoreactivity levels (volume/volume) were determined for each animal.

2.10 Immunohistochemistry and analysis for glutamatergic input marker VGLUT1 at the level of the contralesional cervical spinal cord

2.10.1 Immunohistochemistry for VGLUT1 and NeuN

Vesicular glutamate transporter 1 (VGLUT1) is the major glutamate transporter present in corticospinal cells (Varoqui, Schafer et al. 2002), whereas NeuN serves as a general neuronal marker (a neuronal specific nuclear protein in vertebrates) to aid in locating the ventral horn (Varoqui, Schafer et al. 2002). Cervical spinal cord sections from Sox9^{flox/flox};Cre and Sox9^{flox/flox} mice were incubated with blocking solution (5% goat serum in PBS, with 0.1% Triton X-100) at room temperature for 2 hours, and then incubated with primary antibodies diluted in blocking solution at 4°C overnight. The primary antibodies used were: mouse anti-NeuN (1:200, Millipore, catalogue # MAB377), and rabbit anti-VGLUT1 (1:500, Synaptic Systems, catalogue # 135 302). Sections were washed three times for 10 minutes, after which immunofluorescent labeling was performed using the following secondary antibodies (for one hour at room temperature): Alexa Fluor 488 goat anti-mouse IgG (1:500, Life Technologies, catalogue # A-11029), and Alexa Fluor 594 goat anti-rabbit (1:1000, Life Technologies, catalogue # A-11072). After washing three times in PBS for at least 30 minutes each, the sections were protected with a coverslip using ProLong Gold Anti-Fade mounting medium with DAPI (Life Technologies, catalogue # P36935).

2.10.2 Analysis of glutamatergic input marker VGLUT1 at the level of the contralesional cervical spinal cord

Eight transverse spinal cord sections at the level of the cervical enlargement (at least 100µm apart) were examined to evaluate levels of VGLUT1 within the contralesional cervical spinal cord ventral horns. Images of each section were captured with a 10X objective lens (Olympus BX50). Using Image Pro Plus software, VGLUT1 signal greater than background within the ventral horns was identified and quantified (as area of immunoreactivity/area of ventral horn section). An average VGLUT1 immunoreactivity level (area/area) was determined for each animal.

2.11 Immunohistochemistry and fluorescent microscopy for BDA-labeled fibers at the level of the ipsilesional red nucleus

2.11.1 Immunohistochemistry for BDA-labeled fibers at the level of the ipsilesional red nucleus

Brain sections from Sox9^{flox/flox};Cre mice were incubated with blocking solution (4% goat serum, 1% bovine serum albumin in PBS, with 0.05% Triton X-100) at room temperature for 2 hours, and then incubated with the primary antibody mouse anti-SMI-32 (1:1000, Covance, catalogue # SMI-32R) diluted in blocking solution at 4°C overnight. Sections were washed three times for 10 minutes, after which immunofluorescent labeling was performed using the following secondary antibodies (for one hour at room temperature): Alexa Fluor 488 goat anti-mouse IgG (1:500, Invitrogen, catalogue # A11029), and Streptavidin Alexa Fluor 594 conjugate (1:1000, Invitrogen, catalogue # S-11227). After washing three times in PBS for 10 minutes, 0.5% sudan black in 70% ethanol was applied to the sections for 90 seconds. The sections were rinsed three times for one minute in 70% ethanol, then washed twice for 5 minutes in PBS, and finally protected with a coverslip using ProLong Gold Anti-Fade mounting medium with DAPI (Life Technologies, catalogue # P36935).

2.11.2 Microscopy for BDA- labeled fibers at the level of the ipsilesional red nucleus

Coronal sections at the level of the parvocellular red nucleus within Sox9^{flox/flox};Cre mice (6 weeks post-MCAO) were examined. The objective was to capture a high quality photomicrograph of a BDA-labeled fiber extending to an SMI-32 positive cell in the ipsilesional red nucleus (contralateral to the BDA injection). A 2 µm Z-stack (composed of 10 sections at a thickness of 0.2 µm) was captured with a 60X objective lens on a confocal microscope (Zeiss LSM 510 Meta).

2.12 Statistics

Data are presented as the mean \pm standard error of the mean (SEM). Behavioural test data were analyzed with two-way repeated measures analysis of variance (ANOVA) tests to detect significant effects of genotype and/or time, as well as any interactions. If a significant genotype by time interaction effect was noticed ($p \leq 0.05$), a post-hoc test (Bonferroni) was carried out. Results obtained from the BDA tract tracing experiments were analyzed with Student's t-tests. In both the corticorubral and corticospinal tract analyses, significance was noted when $p < 0.05$. Vesicular glutamate transporter immunohistochemistry results were analyzed with One-way ANOVA tests. If the means were determined to be statistically different, a Newman-Keuls post-hoc test was carried out to detect significant differences between both genotypes at all time points ($p < 0.05$).

Chapter 3:

Results:

3.1 Effects of *Sox9* ablation on functional recovery after MCAO

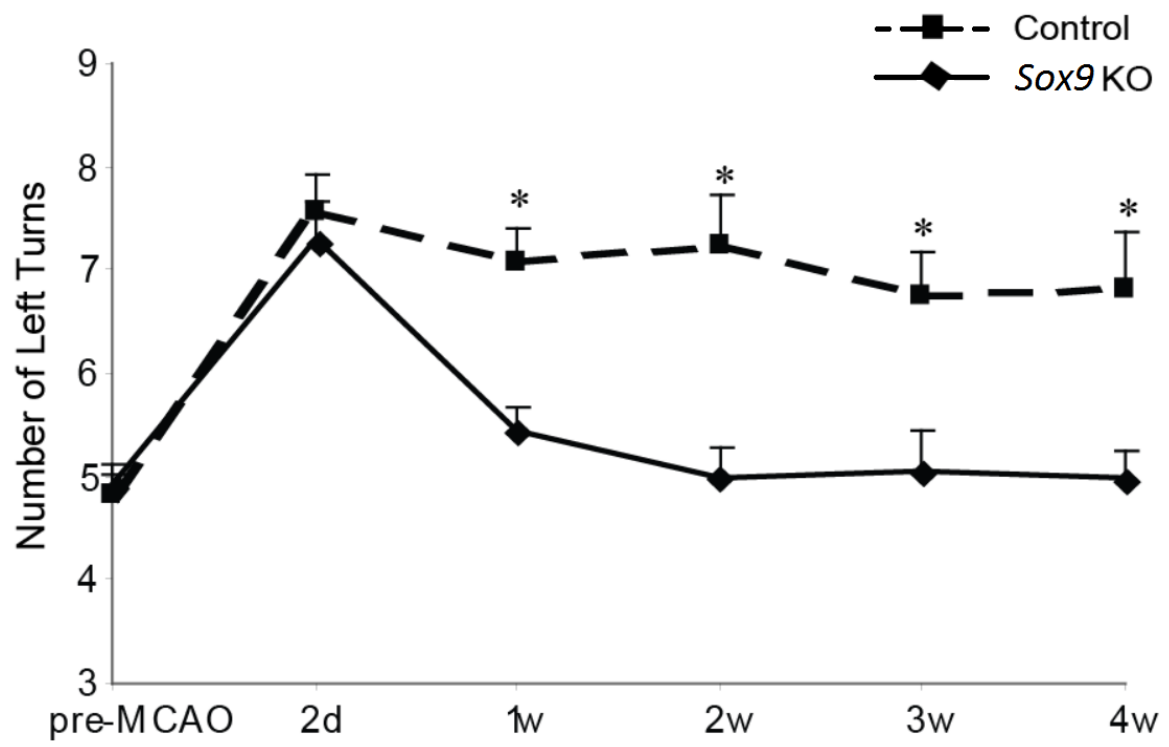
To determine if conditionally knocking out *Sox9* in mice had an effect on functional recovery after MCAO, three separate behavioural tests were used for assessment. After one week of tamoxifen administration, a one week washout period to allow recombination to take place occurred, during which both *Sox9^{flox/flox};Cre* and *Sox9^{flox/flox}* mice underwent pre-testing for sensori-motor function to determine baseline measurements. After being subjected to a 30-minute MCAO injury, neurological recovery of the mice was measured over the subsequent four weeks using the corner, cylinder, and grip strength tests.

3.1.1 Corner test: Sensori-motor recovery after MCAO was improved in *Sox9* knockout mice compared to controls

The corner test was used to detect sensori-motor and postural asymmetries. Before MCAO surgery, control and *Sox9* KO animals made approximately the same number of turns on either side (4.83 ± 0.37 and 4.93 ± 0.195 left turns, respectively). After receiving a left-sided MCAO, all animals displayed an increase in left turns by two days post-surgery. Considerable sensori-motor recovery was seen as early as one week after injury in the *Sox9* KO mice, and by two weeks afterward, they had returned to pre-injury behaviour in which no side preference for turning was noted (7.25 ± 0.494 left turns for controls versus 5 ± 0.277 left turns for *Sox9* KOs). A two-way repeated measures ANOVA test revealed significant effects of genotype and time ($p < 0.0001$), as well as a genotype by time interaction ($p = 0.0024$). Bonferroni post-hoc analyses showed that *Sox9* KO mice experienced significantly improved sensori-motor functional recovery compared to controls on post-MCAO weeks one through four ($p < 0.05$).

Figure 3: *Sox9* KO mice demonstrate improved recovery of sensori-motor function following MCAO as observed in the corner test. All animals subjected to the left-sided MCAO showed an increase in left turns by two days post-surgery. For the *Sox9* KO animals, functional recovery started as early as one week afterwards, and no side preference was noted by the second week. However, in the control group, the progress of functional recovery was much slower. A two-way repeated measures ANOVA revealed significant effects of genotype and time ($p < 0.0001$), as well as a genotype by time interaction ($p = 0.0024$). The * symbol denotes a significant difference between genotypes by a Bonferroni post-hoc test ($p < 0.05$, $n = 12$ for Control, $n = 14$ for *Sox9* KO).

Corner Test



3.1.2 Cylinder test: Sensori-motor recovery after MCAO was improved in *Sox9* knockout mice compared to controls

The cylinder test was also used to examine sensori-motor function in the mice by assessing forelimb use asymmetry. Figure 4 illustrates the cylinder test results obtained between three days to four weeks post-stroke. Preference for placement of the forelimb unaffected by the left-sided MCAO was notable in both groups by three days post-surgery (as indicated by a higher asymmetry score). No preference of forelimb use was observed as early as two weeks after MCAO in the *Sox9* KO mice (asymmetry score of 0.008 ± 0.12). A repeated measurements two-way ANOVA test revealed significant effects of genotype ($p=0.0061$) and time ($p<0.0001$), but no genotype by time interaction. Thus the *Sox9* mice exhibited overall improved sensori-motor functional recovery compared to controls. Pre-MCAO measurements were not recorded for these mice; however, groups of uninjured control and *Sox9* KO mice were tested afterward, to ensure that neither group showed a side preference for turning based solely on genotype ($n=5$ for both control and *Sox9* knockout animals, $p>0.05$ with a Student's t-test; data not shown).

3.1.3 Grip strength test: Recovery of paretic forelimb strength after MCAO was improved in *Sox9* knockout mice compared to controls

The grip strength test was used to assess strength of the paretic right forelimb (innervated by the left hemisphere affected by MCAO). Figure 5 illustrates the grip strength test results obtained before MCAO compared to three days after the surgery, and up to four weeks post-MCAO. Reduction of grip strength was observed in all animals three days after surgery. *Sox9* KO mice managed to attain pre-injury grip strength levels of the paretic limb over the observed testing period (exhibited $96.75 \pm 3.29\%$ of pre-injury strength by four weeks post-MCAO, versus $83.11 \pm 4.43\%$ in the control animals). A repeated measurements two-way ANOVA test revealed a global genotype effect ($p=0.049$) and time effect ($p<0.0001$), but no genotype by time interaction. Thus the *Sox9* mice exhibited overall improved recovery of motor function compared to controls.

Figure 4: *Sox9* KO mice demonstrate improved recovery of sensori-motor function following MCAO as observed in the cylinder test. Main effects of genotype ($p=0.0061$) and time ($p<0.0001$) were observed with a two-way repeated measures ANOVA test. The * symbol denotes the significant effect of genotype ($n=11$ for Control, $n=11$ for *Sox9* KO).

Cylinder Test

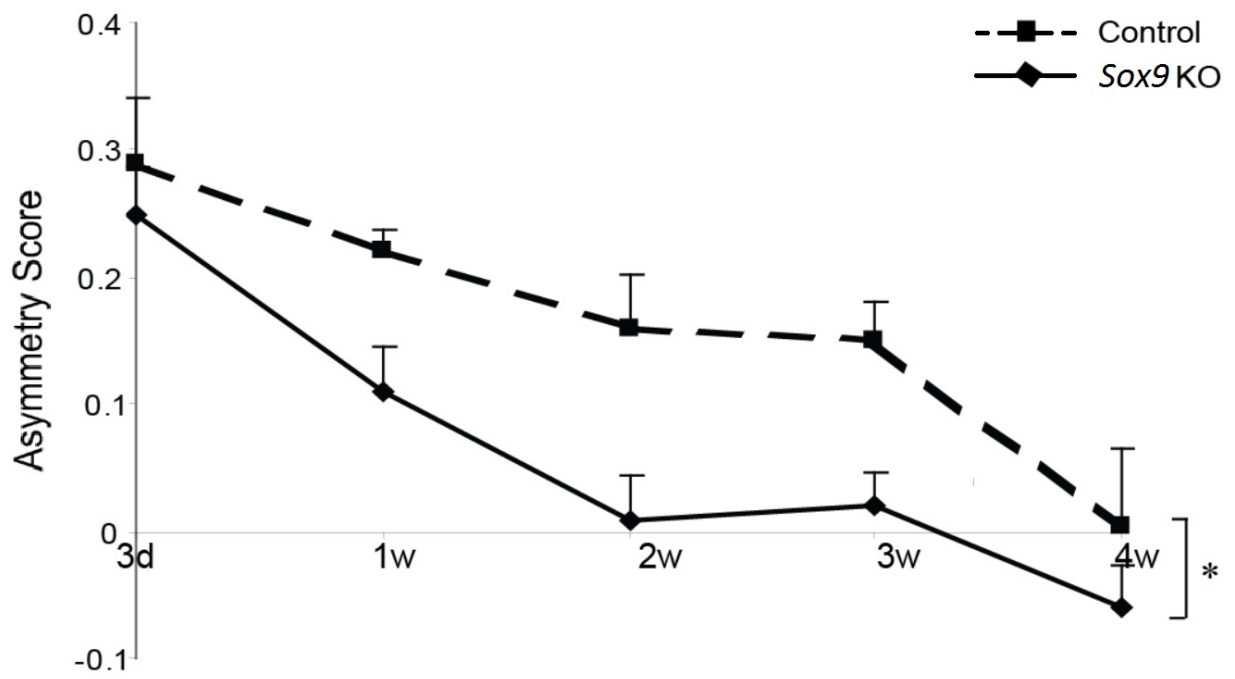
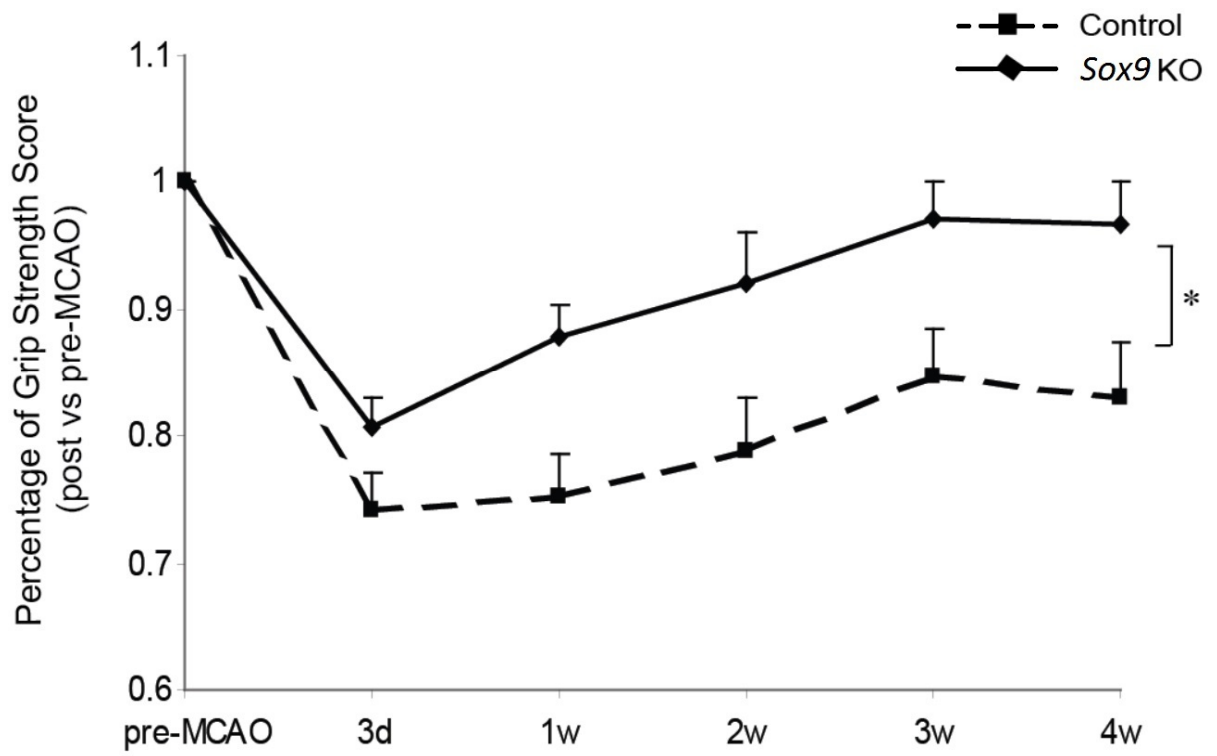


Figure 5: *Sox9* KO mice demonstrate improved recovery of motor function following MCAO as observed in the grip strength test. Main effects of genotype ($p=0.049$) and time ($p<0.0001$) were observed with a two-way repeated measures ANOVA test. The * symbol denotes the significant effect of genotype ($n=9$ for Control, $n=8$ for *Sox9* KO).

Grip Strength Test



3.2 Effects of *Sox9* ablation on structural neuroplasticity after MCAO

To determine if *Sox9* ablation in mice had an effect on structural neuroplasticity after MCAO, a BDA anterograde tract tracing experiment was used to examine the corticorubral and corticospinal tracts originating from the uninjured motor cortex. BDA-labeled fibers present at the level of the red nucleus and cervical spinal cord were examined and counted six weeks after the MCAO injury. The denervated side of the red nucleus was ipsilateral to the MCAO (ipsilesional), since the corticorubral tract innervates primarily ipsilaterally. Tract tracing studies in uninjured rodents show that <1% of fibers cross the midline towards the contralateral red nucleus (when BDA-labeled fiber numbers on the contralateral side are normalized to those within the corticospinal tract) (Z'Graggen, Metz et al. 1998; Reitmeir, Kilic et al. 2011; Herz, Reitmeir et al. 2012). The denervated side of the cervical spinal cord was contralateral to the MCAO (contralesional), since the corticospinal tract innervates primarily contralaterally. Tract tracing studies in uninjured rodents show that only 2-4% of the corticospinal neurons of the sensori-motor cortex project to the ipsilateral spinal cord (Rouiller, Liang et al. 1991). Structural plasticity was assessed by examining numbers of BDA-labeled fibers at the red nucleus and cervical spinal cord to see if *Sox9* ablation led to increased sprouting of motor tract axons into deafferented areas.

3.2.1 *Sox9* ablation led to increased structural plasticity in the contralesional corticorubral tract after MCAO

Anatomical and physiological studies in mice have shown that the red nucleus plays an important role in locomotion through ipsilateral input from the motor cortex, as well as connectivity with the spinal cord, cerebellum, and thalamus (Liang, Paxinos et al. ; Roger and Cadusseau 1987; Jiang, Alheid et al. 2002). Figure 6A is a schematic highlighting the BDA injection into the right motor cortex, and the two corticorubral pathways of interest (with the black line representing normal innervation, and the dotted line extending to the denervated side). BDA-labeled fibers at the level of the parvocellular red nucleus on both sides were quantified six weeks post-MCAO.

Our results revealed significantly higher numbers of BDA-labeled corticorubral fibers present at the ipsilesional (deafferented) red nucleus in *Sox9* KO mice by a Student's t-test ($p < 0.05$, average of 3.5 ± 1.402 fibers for controls and 11.36 ± 1.588 fibers for *Sox9* KO mice). In order to control for labeling efficiency differences among animals, this number was normalized to the number of BDA-labeled fibers present on the contralesional side (which were not significantly different between *Sox9* KO and control animals). The resulting percentages of BDA-labeled corticorubral fibers present on the ipsilesional side six weeks post-MCAO were significantly higher in the *Sox9* KO mice compared to control animals. These results suggest increased structural plasticity in the intact corticorubral tract (contralesional) after MCAO in *Sox9* KO animals. Figure 7 depicts two high quality confocal images of BDA-labeled fibers extending to SMI-32 positive cells (representative of rubrospinal cells) at the denervated parvocellular red nucleus in *Sox9* KO mice.

Figure 6: *Sox9* KO mice display increased contralesional corticorubral neuroplasticity after MCAO compared to control animals.

A) Biotinylated dextran amine (BDA) was injected into the contralesional motor cortex and BDA-labeled fibers were quantified at the level of the parvocellular red nucleus (RN).

(B-E) Photomicrographs of representative parvocellular red nucleus sections from control and *Sox9*-ablated mice six weeks after MCAO, both contralateral and ipsilateral to the BDA injection. Scale bar in B, D = 25 μ m. Scale Bar in C, E = 100 μ m.

(F) Quantification of the number of BDA-stained fibers present at the ipsilesional parvocellular red nucleus. The *Sox9*-ablated mice exhibited significantly higher numbers of BDA-labeled fibers on the denervated side compared to control mice as demonstrated by a Student's t-test ($p < 0.05$, $n = 6$ for Control, $n = 8$ for *Sox9* KO). **(G)** Percentages of BDA labeled fibers present at the denervated ipsilesional parvocellular red nucleus (number of BDA-labeled fibers extending to denervated side normalized to the number of BDA-labeled fibers on the contralesional side). The *Sox9*-ablated mice exhibited significantly higher percentages of BDA-labeled fibers on the denervated side compared to control mice as demonstrated by a Student's t-test ($p < 0.05$, $n = 6$ for Control, $n = 8$ for *Sox9* KO).

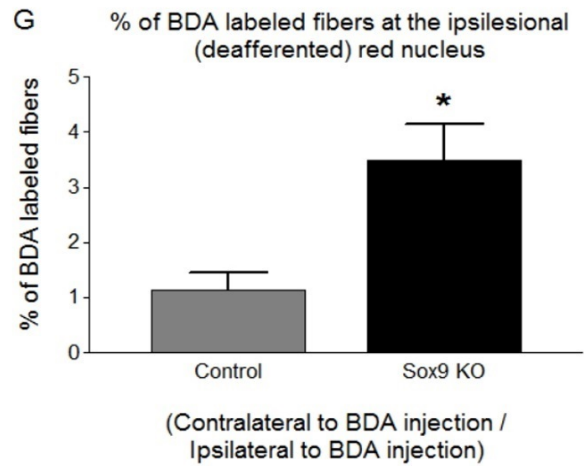
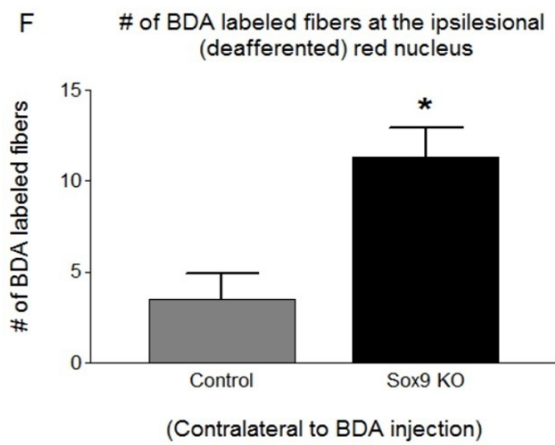
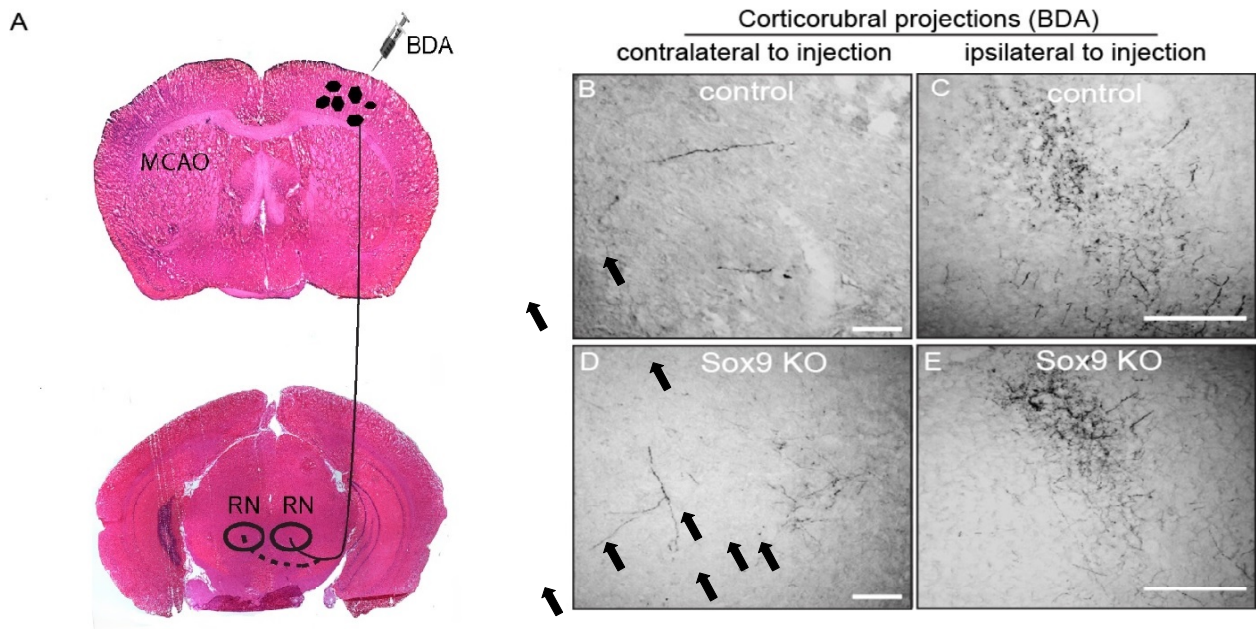
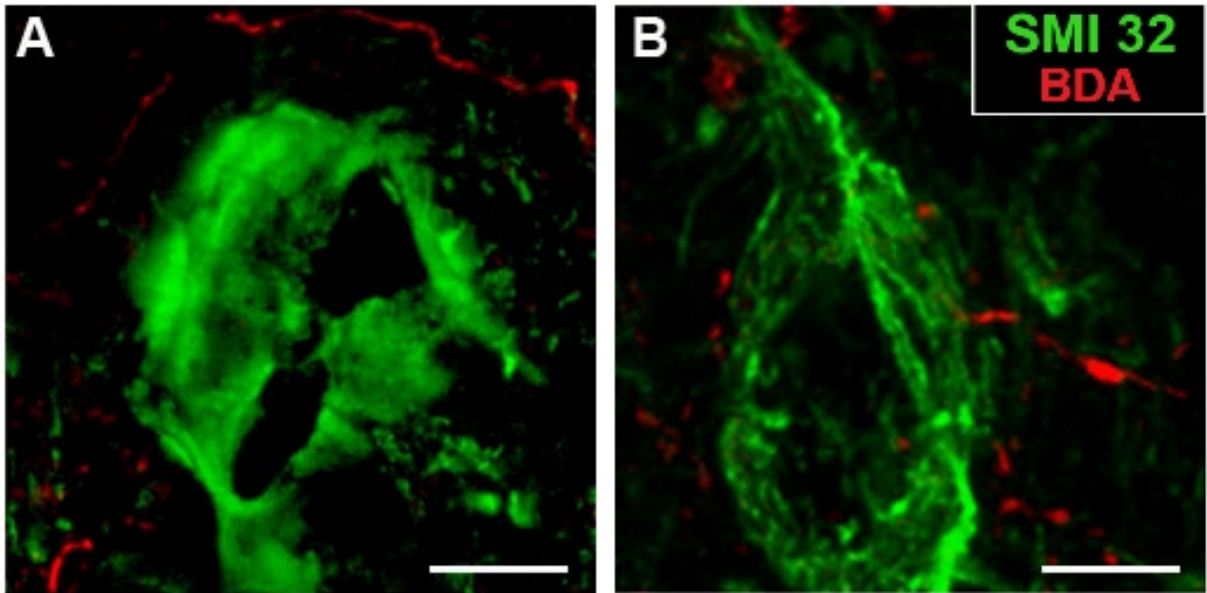


Figure 7: Confocal photomicrographs depicting BDA-labeled fibers extending to SMI-32 positive cells at the denervated (ipsilesional) parvocellular red nucleus. (A,B) Two photomicrographs of representative ipsilesional red nucleus SMI-32 positive cells from *Sox9*-ablated mice 6 weeks after MCAO. BDA fibers shown in red are from neurons originating in the contralateral motor cortex. Scale bar in A-B = 5 μ m.



3.2.2 *Sox9* ablation led to increased structural plasticity in the contralesional corticospinal tract after MCAO

In the corticospinal tract (CST), long axons of the cortical pyramidal neurons decussate almost completely at the pyramidal decussation within the brainstem, and over 90% of fibers project via the dorsal funiculus, to the contralateral half of the spinal cord (Rouiller, Liang et al. 1991). Figure 8A is a schematic highlighting the BDA injection into the right motor cortex, and the two corticospinal pathways of interest (with the black line representing normal innervation, and the dotted line extending to the denervated side). Injection of BDA into the right (contralesional) side of the sensori-motor cortex resulted in clear positive staining in the dorsal funiculus of the left (ipsilesional) side of the spinal cord. BDA-staining at the level of cervical enlargement in the ipsilesional spinal cord (predominantly innervated side) showed no significant difference between *Sox9* KO and control groups.

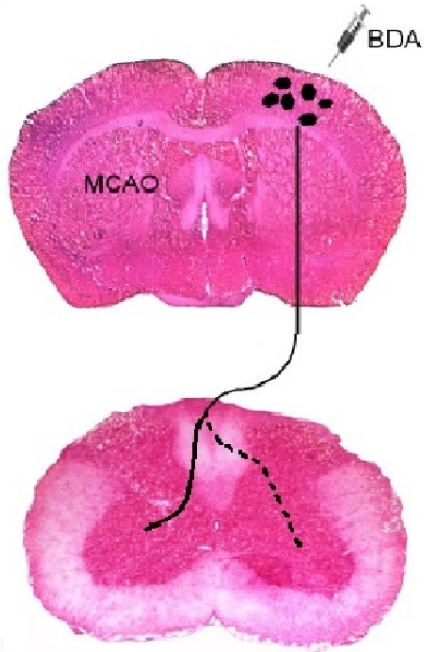
Our results revealed significantly higher numbers of BDA-labeled fibers present at the contralesional (deafferented) side of the cervical spinal cord in the *Sox9* KO mice by a Student's t-test ($p < 0.05$, average of 9.417 ± 2.173 fibers for controls and 19.06 ± 2.325 fibers for *Sox9* KO mice). In order to control for labeling efficiency differences among animals, this number was normalized to the number of BDA-labeled fibers on the ipsilesional side. The resulting percentages of BDA-labeled fibers present within the deafferented contralesional cervical spinal cord were also significantly higher in the *Sox9* KO mice compared to control animals ($p < 0.05$). These results suggest increased structural plasticity in the contralesional corticospinal tract after MCAO in *Sox9* KO animals.

Figure 8: *Sox9* KO mice display increased contralesional corticospinal neuroplasticity after MCAO compared to control animals.

(A) Biotinylated dextran amine (BDA) was injected into the contralesional motor cortex and BDA-labeled fibers were quantified at the level of the cervical spinal cord.

(B-E) Photomicrographs of representative cervical spinal cord sections from control and *Sox9*-ablated mice six weeks after MCAO, both contralateral and ipsilateral to the BDA injection. Scale bar in B, D = 100 μ m. Scale bar in C, E = 25 μ m (F) Quantification of the number of BDA-stained fibers crossing the midline to the contralesional cervical spinal cord. The *Sox9*-ablated mice exhibited significantly higher numbers of BDA-labeled fibers on the denervated side compared to control mice as demonstrated by a Student's t-test ($p < 0.05$, $n = 6$ for Control, $n = 8$ for *Sox9* KO). (G) Percentages of BDA labeled fibers present within the denervated, contralesional side of cervical spinal cord (number of BDA-labeled fibers extending to denervated side normalized to the number of BDA-labeled fibers on the ipsilesional side). The *Sox9*-ablated mice exhibited significantly higher percentages of BDA-labeled fibers on the denervated side compared to control mice as demonstrated by a Student's t-test ($p < 0.05$, $n = 6$ for Control, $n = 8$ for *Sox9* KO).

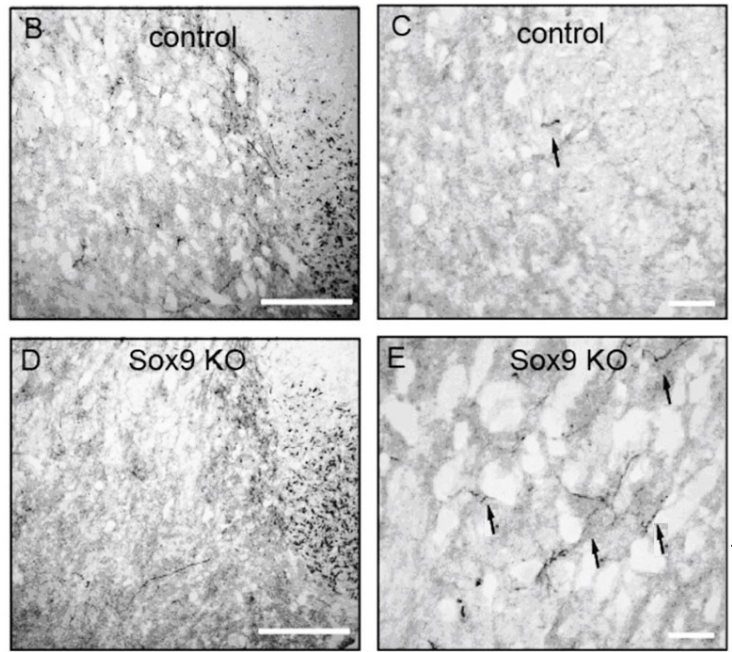
A



Corticospinal projections (BDA)

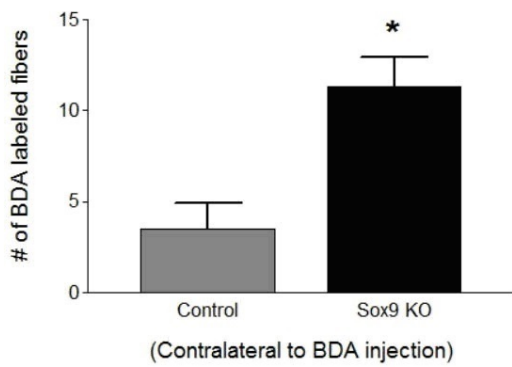
contralateral to injection

ipsilateral to injection



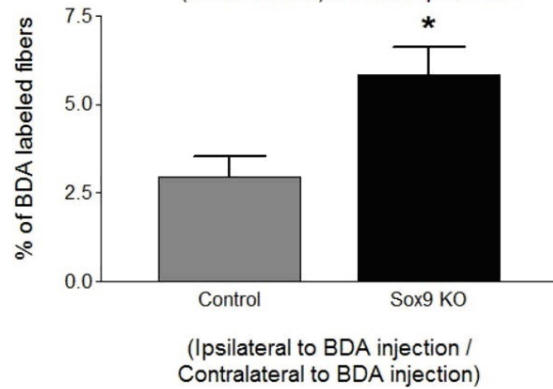
F

of BDA labeled fibers at the contralesional (deafferented) cervical spinal cord



G

% of BDA labeled fibers at the contralesional (deafferented) cervical spinal cord



3.3 Effects of *Sox9* ablation on putative synaptic plasticity after MCAO

To determine if *Sox9* ablation in mice had an effect on synaptic neuroplasticity after MCAO, immunohistochemistry was used to examine glutamatergic input markers at the deafferented red nucleus and ventral horn of the cervical spinal cord. Vesicular glutamate transporter 1 (VGLUT1) is the major glutamate transporter of corticorubral cells, while VGLUT2 is the major glutamate transporter of cerebellar inputs (Allen Brain Atlas - VGlut1 in mouse brain; Allen Brain Atlas - VGlut2 in mouse brain; Varoqui, Schafer et al. 2002; Fink, Englund et al. 2006). Thus, it was of interest to see if levels of these important glutamatergic markers differed between genotypes, and if they correlated with the structural neuroplasticity data. VGLUT1 and/or VGLUT2 levels within the denervated red nucleus and cervical spinal cord were examined and counted six weeks after sham surgeries, as well as 48 hours and six weeks after the MCAO injury in both groups of animals. VGLUT levels were assessed to determine if *Sox9* ablation led to increased levels of glutamatergic synaptic markers (and theoretically, increased innervation) within deafferented areas.

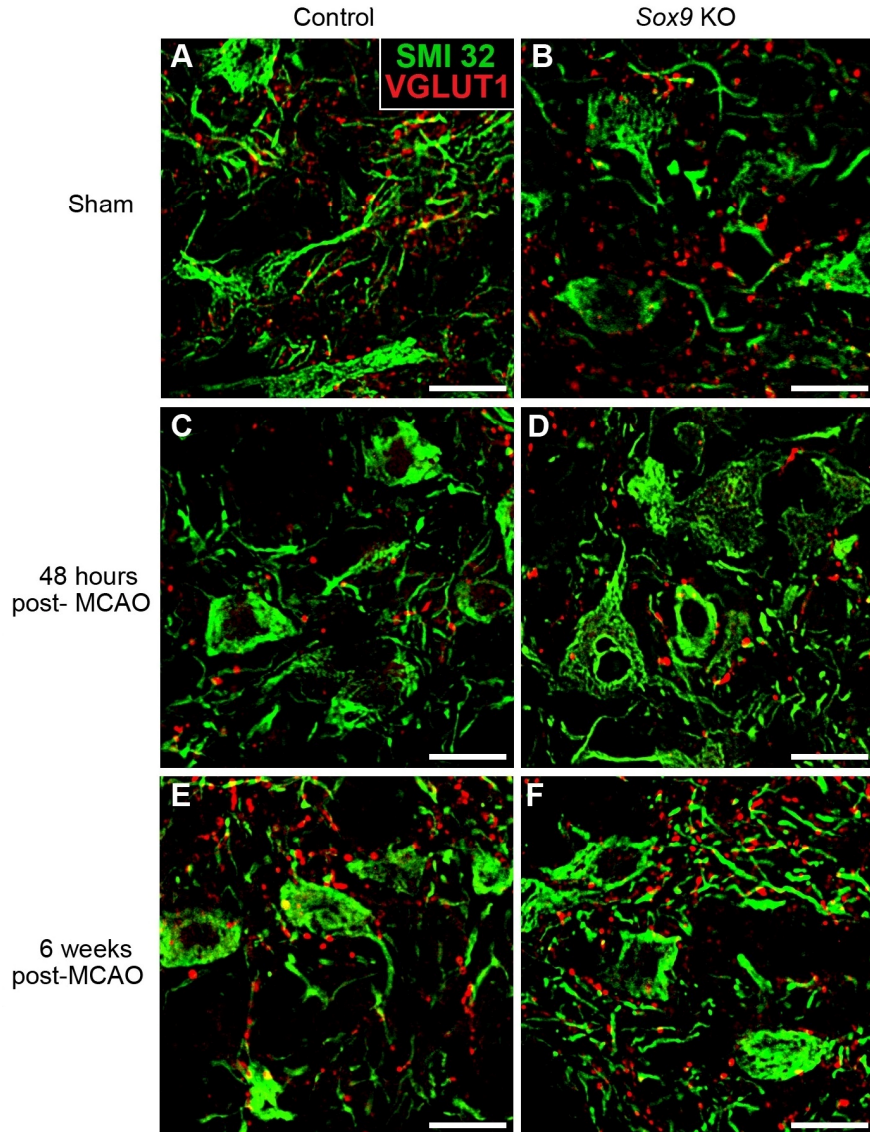
3.3.1 *Sox9* ablation led to increased levels of VGLUT1 input markers at the deafferented red nucleus six weeks after MCAO

Results of a One-way ANOVA followed by a Newman-Keuls post-hoc test (Figure 9) revealed that 48 hours after MCAO, both control and *Sox9* KO animals experienced a significant loss in VGLUT1 immunoreactivity at the deafferented, ipsilesional parvocellular red nucleus compared to sham animals (symbolized by statistically difference groups "a" and "b" on in Figure 9). Sham animals were included to represent normal VGLUT1 levels. However, six weeks after MCAO, *Sox9*-ablated animals displayed increased VGLUT1 immunoreactivity levels (statistically the same level as the Sham animals exhibited, denoted by the label "a" in the figure). The control mice also experienced a significant increase in VGLUT1 levels at the ipsilesional red nucleus from 48 hours to six weeks-post MCAO (label "c" in Figure 9), but this was significantly lower than that measured in the sham animals and the six weeks post-MCAO *Sox9* KO mice.

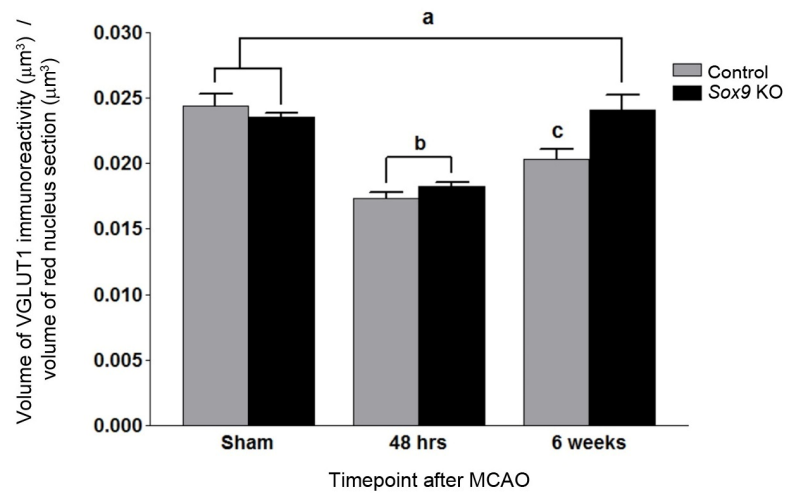
Figure 9: *Sox9* KO mice display increased levels of VGLUT1 at the ipsilesional red nucleus six weeks post-MCAO compared to control animals, after a significant decrease in both groups 48 hours-post MCAO compared to shams.

Representative photomicrographs of parvocellular red nucleus sections ipsilateral to MCAO from control and *Sox9*-ablated mice six weeks after a sham surgery (**A, B**), 48 hours after MCAO (**C, D**), and six weeks after MCAO (**E, F**). Vesicular glutamate transporter 1 (VGLUT1) in red represents glutamatergic input mainly from the motor cortex. SMI-32 in green represents rubrospinal neurons. Bar in A-F = 20 μ m.

(G) Quantified volume of VGLUT1 immunoreactivity per volume of red nucleus section for each animal type, and time point. There was a significant decrease in VGLUT1 immunoreactivity between Sham animals and 48 hours post-MCAO animals for both groups. However, *Sox9*-ablated animals displayed increased VGLUT1 immunoreactivity levels six weeks after MCAO (attain same level as the Sham animals exhibit), whereas the control mice did not increase back to this normal level. The different letters a, b, and c represent significantly different groups by One-way ANOVA, followed by a Newman-Keuls post-hoc test ($p < 0.05$, $n=3$ for Sham-Control and 48 hours-*Sox9* KO, $n=4$ for Sham-*Sox9* KO, $n=5$ for 48 hours-*Sox9* KO and 6 weeks-Control, $n=6$ for 6 weeks-*Sox9* KO).



G Quantification of VGLUT1 in ipsilesional red nucleus



3.3.2 *Sox9* ablation did not lead to increased levels of VGLUT2 input markers at the deafferented red nucleus six weeks after MCAO

Results of a One-way ANOVA followed by a Newman Keuls post-hoc test (Figure 10) revealed that there were no significant differences between control and *Sox9* KO animals at any individual time point. Sham animals were included to represent normal VGLUT2 levels. However, 48 hours after MCAO, control animals experienced a significant loss in VGLUT2 immunoreactivity at the deafferented, ipsilesional red nucleus compared to sham animals. Both *Sox9* KO and control animals exhibited significantly increased levels of VGLUT2 from 48 hours post-MCAO to six weeks after injury ($p < 0.05$), but were statistically equivalent at the six weeks post-MCAO time point.

3.3.3 *Sox9* ablation did not significantly change levels of VGLUT1 input markers at the deafferented cervical spinal cord ventral horn six weeks after MCAO

Results of a One-way ANOVA revealed that VGLUT1 levels at the deafferented, contralesional cervical spinal cord ventral horn did not differ significantly between sham or six weeks post-MCAO animals in *Sox9* KO or control groups (Figure 11, $p > 0.05$).

Figure 10: *Sox9* KO mice exhibit no significant loss of VGLUT2 levels at the ipsilesional red nucleus 48 hours post-MCAO compared to sham animals, and both *Sox9* knockout and control animals experience significantly increased levels of VGLUT2 by six weeks afterwards.

Representative photomicrographs of ipsilesional parvocellular red nucleus sections from control and *Sox9*-ablated mice six weeks after a sham surgery (**A, B**), 48 hours after MCAO (**C, D**), and six weeks after MCAO (**E, F**). Vesicular glutamate transporter 2 (VGLUT2) in red represents glutamatergic input from other CNS areas (cerebellar and thalamic). SMI-32 in green represents rubrospinal neurons. Bar in A-F = 20 μ m.

(G) Quantified VGLUT2 volume of immunoreactivity per volume of red nucleus section for each animal type, and time point. There were no significant differences in VGLUT2 immunoreactivity levels between control and *Sox9* KO animals at any individual time point. There were also no significant differences between Sham and six weeks-post MCAO groups (for control and *Sox9* KO animals); However, at 48 hours post-MCAO, control animals displayed a significant decrease in VGLUT2 immunoreactivity at the level of the deafferented parvocellular red nucleus compared to both types of Sham animals, whereas the *Sox9* KO animals at 48 hours post-MCAO did not. At six weeks post-MCAO, both control and *Sox9* KO animals displayed significantly increased VGLUT2 levels (statistically equal to Sham, showing normal levels) compared to their counterparts at 48 hours-post MCAO. The * symbol represents a significant difference between two groups by One-Way ANOVA, followed by a Newman-Keuls post-hoc test ($p < 0.05$, $n=3$ for Sham-Control, Sham-*Sox9* KO, and 48 hours-*Sox9* KO, $n=5$ for 48 hours-Control and 6 weeks-Control, $n=6$ for 6 weeks-*Sox9* KO).

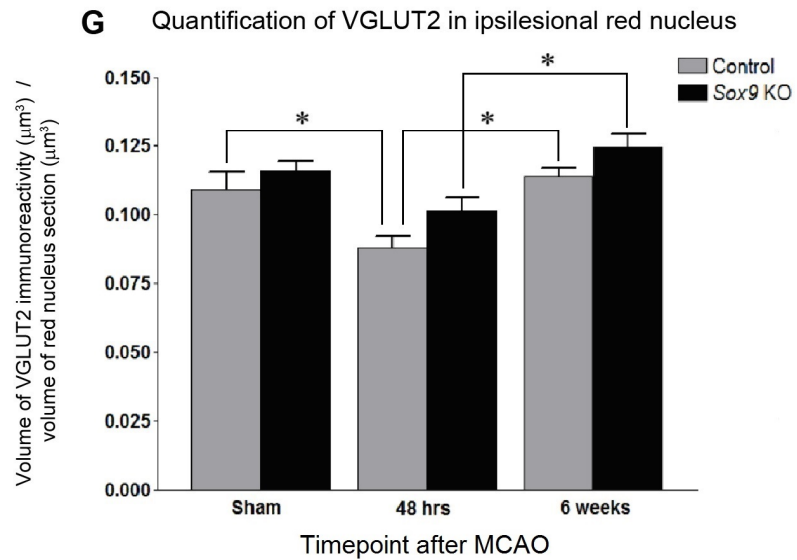
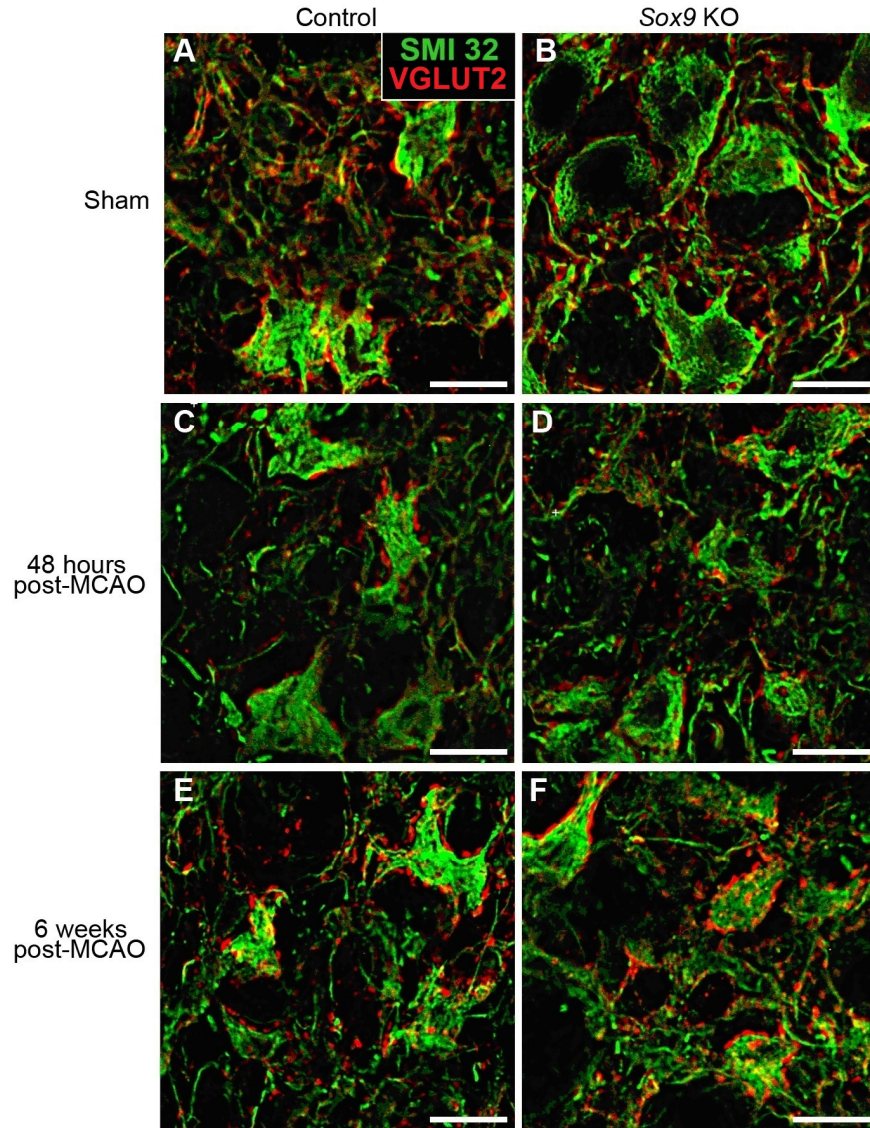
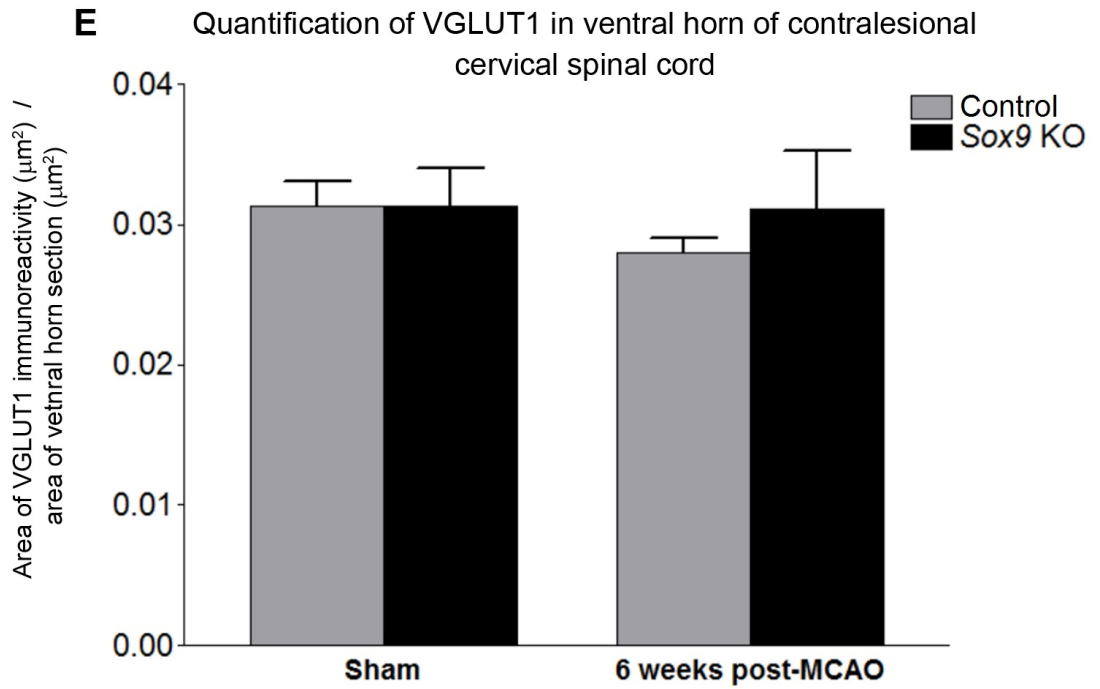
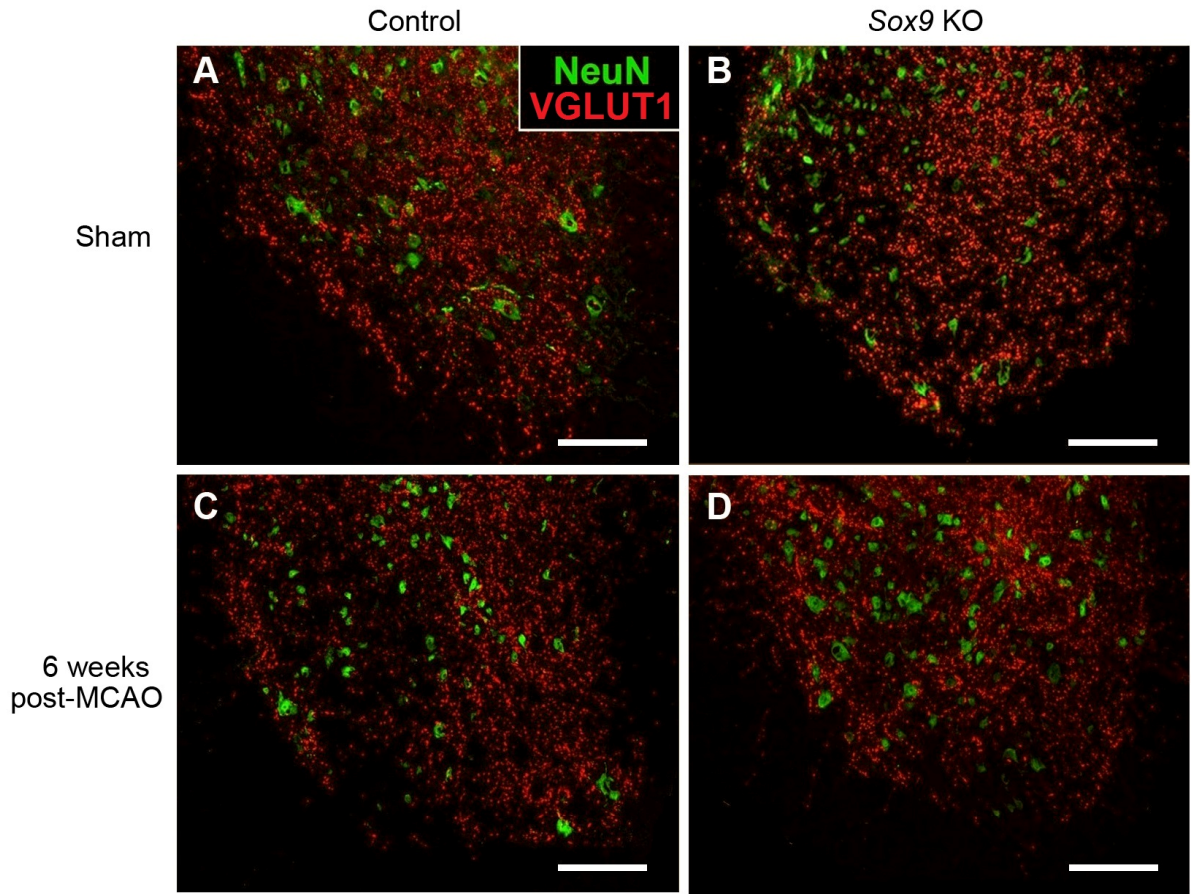


Figure 11: VGLUT1 levels at the contralesional cervical spinal cord ventral horn do not differ significantly between sham or six weeks post-MCAO animals in either *Sox9* KO or control groups.

Representative photomicrographs of contralesional cervical spinal cord ventral horn sections from control and *Sox9*-ablated mice six weeks after a sham surgery (**A, B**), and six weeks after MCAO (**C, D**). Vesicular glutamate transporter 1 (VGLUT1) in red represents glutamatergic input mainly from the motor cortex. NeuN in green is a marker for nuclei of neurons; large motor neurons of the ventral horn are evident. Bar in A-D = 100 μ m. (**E**) Quantified VGLUT1 area of immunoreactivity per area of cervical spinal cord ventral horn section for each animal type, and time point. There were no significant differences in VGLUT1 immunoreactivity levels between the different groups of animals as determined by a One-Way ANOVA ($p > 0.05$, $n=4$ for Sham-Control and Sham-*Sox9* KO, $n=5$ for 6 weeks-*Sox9* KO, $n=6$ for 6 weeks-Control).



Chapter 4:

Discussion

This research project aimed to enhance understanding of the role of the transcription factor SOX9 in stroke pathology and recovery. Having previously identified SOX9 as responsible for upregulating the expression of axonal growth-inhibiting CSPGs in the injured CNS, we hypothesized that decreasing levels of SOX9 would result in increased neuroplasticity, and in turn, improved functional recovery after stroke in mice. To achieve this, we used a conditional knockout mouse model in which exons 2 and 3 of the *Sox9* were removed with a Cre-loxP system, inducible by tamoxifen administration. It is pertinent to note that in this model, *Sox9* would theoretically be knocked out in all cell types.

4.1 The influence of SOX9 on functional recovery after stroke

The first objective of my thesis was to determine whether or not conditionally knocking out *Sox9* would alter functional recovery after stroke in mice. Three separate behavioural tests were implemented to assess neurological and motor function after MCAO. Used to detect sensori-motor and postural asymmetries, the corner test results displayed perhaps the most significant example of improved sensori-motor recovery after stroke in the *Sox9*-ablated mice compared to control animals. *Sox9* KO mice were exhibiting pre-injury behaviour of no side preference for turning by two weeks after MCAO, whereas the control animals displayed significantly slower progress and lower levels of sensori-motor recovery over the four post-injury weeks. The corner test is known to be one of most reliable tests for detecting long-term sensori-motor dysfunction in rodents after injury (Zhang, Schallert et al. 2002). Thus, it was encouraging that the results to this sensitive test revealed the most prominent significant differences between *Sox9* KO and control animals out of all behavioural tests (significant effects of genotype and time, as well as genotype-time interactions on all post-surgical weeks).

Other important markers of functional recovery after stroke include use and strength of the paretic limb. The cylinder test results demonstrated overall improved functional recovery after MCAO in *Sox9* KO mice compared to control animals, with significant effects of both genotype and time in forelimb use asymmetry over the four week post-surgical testing period. The results also suggested that *Sox9* KO mice used the unaffected and paretic forelimbs equally to explore the cylinder wall by two weeks after MCAO (asymmetry score of 0.008 ± 0.12). The grip strength test highlighted significantly improved recovery in strength of the paretic limb in the *Sox9*-ablated animals compared to controls animals, with a significant effect of both genotype and time. The data suggested that *Sox9* KO animals achieved full recovery of grip strength ($96.8 \pm 3.3\%$) by the end of the testing period.

The general trend seen with the behavioural test data confirmed our hypothesis that the *Sox9* KO would display improved functional recovery after MCAO compared to control animals. It is of interest to note that mice, in general, experience endogenous recovery to a remarkable degree after stroke (in comparison to humans). It is a unique characteristic of the lissencephalic rodent brain that allows mice to survive larger strokes in considerable numbers (Carmichael 2005). Along with higher survival rates, the time-course of post-stroke recovery is often much shorter in rodents than in humans (Murphy and Corbett 2009). This implies that decreasing levels of SOX9 within the mice improved and augmented the already relatively high levels of endogenous sensori-motor recovery. It is possible that decreasing levels of SOX9 affects a few different processes that, in combination, produce significant functional improvements seen in the ubiquitous *Sox9* knockout mice. As discussed in the introduction, ample evidence in the literature (and work completed by our research group) led to our hypothesis that lower SOX9 levels, and in turn lower CSPG levels, could result in increased neuroplasticity. Therefore, after behavioural testing, examining neuroplasticity in these animals was our primary focus.

4.2 The influence of SOX9 on neuroplasticity after stroke

The two main mechanisms for neuroplastic change and reorganization after stroke are thought to be the formation of new neuronal circuitry, and the unmasking/strengthening of existing pathways (Soleman, Yip et al. 2012). Thus the second objective of my thesis was to evaluate structural and synaptic neuroplasticity after MCAO in mice, and compare between *Sox9*-ablated mice and controls. There are many ways to assess neuroplasticity; however, the two methods used in this work were tract-tracing of the contralesional corticorubral and corticospinal pathways, as well as immunohistological quantification of glutamatergic input synaptic markers at deafferented CNS areas relevant to motor function.

4.2.1 Examination of structural neuroplasticity after stroke

Tract-tracing findings supported our hypothesis that the *Sox9*-ablated mice would exhibit increased structural neuroplasticity after MCAO compared to controls. I examined labeled axons of neurons originating in the uninjured side of the sensori-motor cortex, and focused on two areas of descending projections that are very relevant to motor function: the red nucleus in the midbrain and cervical enlargement of the spinal cord. The literature shows that in control animals, these predominantly unilateral connections become increasingly bilateral after stroke, as contralesional corticofugal axons sprout to innervate deafferented areas (Lee, Kim et al. 2004; Zai, Ferrari et al. 2009).

In the present study, significantly higher numbers (and overall percentages, when controlling for labeling efficiency) of BDA-labeled fibers were found within the deafferented red nuclei and cervical spinal cords of the *Sox9* KO animals compared to controls animals six weeks after MCAO. This indicates that conditionally knocking out *Sox9* significantly enhanced the endogenous structural plasticity of the contralesional corticorubral and corticospinal tracts seen in control animals. This is likely due to a) increased sprouting of contralaterally projecting corticorubral axons that normally contribute only minimally (<1%) to corticorubral inputs (Z'Graggen, Metz et al. 1998;

Reitmeir, Kilic et al. 2011; Herz, Reitmeir et al. 2012), and b) increased sprouting of ipsilaterally projecting corticospinal axons that normally contribute only minimally (2-4%) to corticospinal inputs (Rouiller, Liang et al. 1991).. The growth of corticofugal fibers across the midline to reach deafferented areas may still be a formal possibility; however, sprouting of uninjured axons that were already within the deafferented areas may be more likely to contribute to the improved function recovery of the *Sox9* KO mice, since axon growth is a relatively slow process (Cho, Yang et al. 2005).

Whether it was an increase in collateral connections, or an elaboration of unilateral connections to the denervated areas that were present before injury, increased contralesional corticofugal structural neuroplasticity was observed in the *Sox9* KO animals compared to controls. We hypothesize that this was due to the consequently lower levels of CSPGs (both in the diffuse extracellular matrix and dense peri-neuronal nets) in the knockout animals, which would have theoretically created a CNS environment more permissive to axon sprouting. The increased structural plasticity of uninjured corticofugal fibers may have contributed to the improved functional recovery observed in the *Sox9* KO mice. Further studies might include electrophysiological experiments to determine whether or not this increased fiber growth into deafferented area does, in fact, translate into increased functionality.

4.2.2 Examination of synaptic neuroplasticity after stroke: glutamatergic input markers at the denervated red nucleus

If the improved functional recovery observed in the *Sox9* KO mice is due the increased reactive sprouting of corticofugal projections (demonstrated by the BDA-labeling) , then one would predict that the *Sox9* KO mice would also demonstrate increased expression levels of synaptic proteins in the deafferented red nucleus and cervical spinal cord compared to controls. Thus, we examined the expression levels of presynaptic markers in the ipsilesional red nucleus and contralesional cervical spinal cord. The literature suggests that VGLUT expression is used endogenously to directly regulate the extent of glutamate release, which presents a presynaptic mechanism to

control excitatory transmission for synaptic refinement and plasticity (Wilson, Kang et al. 2005). Therefore, a change in presynaptic VGLUT levels suggests a change in excitatory innervation. The quantification of synaptic markers has been used in other central nervous system injury studies to examine probable changes in innervation at deafferented areas (e.g. the spinal cord) (Apostolova, Irintchev et al. 2006; Zhao, Zhao et al. 2013). Our tract tracing findings displayed an increase in fibers projecting from the uninjured sensori-motor cortex to the deafferented parvocellular red nucleus in the *Sox9* KO animals, so it was of interest to see if this corresponded with an increase in VGLUT expression.

As discussed in the introduction, the corticorubral tract is composed of glutamatergic neurons, with VGLUT1 as the predominantly expressed vesicular glutamate transporter (Allen Brain Atlas -VGlut1 in mouse brainBromberg, Penney et al. 1981). The immunohistological analysis revealed that both *Sox9* KO and control mice experienced loss of VGLUT1 levels at the deafferented parvocellular red nucleus by 48 hours post-MCAO. The small, however significant, increase in VGLUT1 levels exhibited by the control animals at six weeks post-MCAO testifies to the neuroplasticity that normally occurs post-stroke. The *Sox9* KO mice exhibited full restoration of VGLUT1 levels by six weeks post-MCAO (statistically equivalent to sham levels), which suggests a heightened level of neuroplasticity in these mice compared to controls. The significantly higher VGLUT1 levels at the deafferented red nucleus in the knockout animals corresponded with an increased presence of fibers projecting from the contralesional sensori-motor cortex. Again, we hypothesize that this occurred due to lower levels of CSPGs (both in diffuse extracellular matrix and dense peri-neuronal nets), which created a CNS environment more permissive to neuroplasticity and synapse formation.

Further experiments may include co-staining for BDA and VGLUT1 at the deafferented parvocellular red nucleus. Co-localization would suggest that the contralesional corticorubral fibers expressed the presynaptic glutamatergic transporter proteins necessary to make functional connections with deafferented neurons. Another useful experiment to further provide evidence of putative functional synapses would

involve co-staining for presynaptic VGLUT1 proteins and corresponding post-synaptic density proteins (PSD). PSD-95 is the most ubiquitous and best characterized of the glutamatergic PSD proteins, and is thought to be fundamentally important in anchoring AMPA (α -Amino-3-hydroxy-5-methyl-4-isoxazolepropionic acid) receptors at the post-synaptic membrane (Bruneau, Esteban et al. 2009). Since proper post-synaptic protein expression is also essential to synapse functionality, co-localization of VGLUT1 and PSD-95 at cell membranes of interest would further suggest potential synapse functionality. Again, electrophysiological studies would be ideal to reinforce this hypothesis, and confirm the existence of functional connections.

VGLUT2 levels at the deafferented red nucleus tell a somewhat different story. Another major glutamatergic input to the red nucleus extends from the deep cerebellar nuclei of the cerebellum; these projections are predominantly VGLUT2-positive (Allen Brain Atlas - VGlut2 in mouse brain; Fink, Englund et al. 2006). Efferent projections to the parvocellular red nucleus also extend from the posterior thalamic nuclei. Since VGLUT2 has been established as the most abundant VGLUT isoform of thalamic nuclei, this is likely a source of VGLUT2 innervation as well (Moechars, Weston et al. 2006; Barroso-Chinea, Castle et al. 2007). Together, cerebellar and thalamic glutamatergic innervation at the red nucleus play a role in movement coordination and proper integration of sensori-motor information (Roger and Cadusseau 1987; Siegel 2010)

Immunohistological analysis revealed that only control animals experienced a significant decrease in VGLUT2 levels at the deafferented red nucleus by 48 hours after stroke. Since the red nucleus and cerebellum are both in areas of the brain that are not directly damaged by MCAO, it is unlikely that this loss of VGLUT2 levels was due to lost cerebellorubral connections. The thalamus does not receive direct blood supply from the MCA either; however, it is supplied by branches of the internal carotid artery, which is a vessel manipulated during the MCAO procedure. This, in combination with its relative proximity to the infarcted area, may have put the thalamus at risk for damage from ischemia or secondary processes (Popp, Jaenisch et al. 2009). As such, there is a chance that some degree of ischemic damage occurred, leading to a slight decrease in thalamorubral VGLUT2-positive input to the red nucleus. In the *Sox9* KO animals, there

was no significant decrease in VGLUT2 input at 48 hours post-MCAO, which may have been due to some sort of neuroprotective effect caused by *Sox9* ablation. However, similar evidence for neuroprotection was not observed in the VGLUT1 analyses. In any case, it would be advantageous to complete future experiments to examine the possibility of neuroprotection (such as retrograde tract tracing from deafferented areas) and compare between genotypes.

Finally, both *Sox9* KO and control animals experienced a significant increase in VGLUT2 levels at the deafferented parvocellular red nucleus from 48 hours after injury to reach normal levels by six weeks post-MCAO. In the control animals, this may have once again been due to endogenous levels of neuroplasticity. Since the control animals did not attain normal levels of VGLUT1 expression at the deafferented red nucleus by six weeks after MCAO, an increase in excitatory innervation from other areas may have been a more needed and encouraged compensatory response. The lack of a significant difference between control and *Sox9* KO animals by six weeks after MCAO may indicate that VGLUT2-positive innervation (most likely of thalamic and cerebellar origin) at the deafferented red nucleus did not play a major role in the improved functional recovery seen in the knockout animals.

4.2.3 Examination of synaptic neuroplasticity after stroke: glutamatergic input markers at the denervated cervical spinal cord ventral horn

As discussed in the introduction, the corticospinal tract is composed of glutamatergic neurons, with VGLUT1 as the predominant vesicular glutamate transporter expressed (Allen Brain Atlas -VGlut1 in mouse brain Bromberg, Penney et al. 1981; Varoqui, Schafer et al. 2002). The immunohistological analysis of VGLUT1 levels at the deafferented cervical spinal cord ventral horn revealed that there were no significant differences between control or *Sox9* KO animals six weeks post-MCAO. VGLUT1 levels at six weeks-post MCAO in both groups of mice were also statistically equivalent to those exhibited by sham animals. It is interesting to note that, unlike the VGLUT1 immunohistochemistry analysis at the red nucleus, this data does not correlate with the tract tracing findings; the BDA experiments showed that more fibers from the

contralesional cortex were present within the deafferented cervical spinal cord in the *Sox9* KO animals six weeks after MCAO compared to controls.

This may have resulted for a number of reasons. It is possible that other glutamatergic inputs to the deafferented cervical spinal cord ventral horn played a role in the improved functional recovery seen in the knockout animals. Since putative contralesional corticorubral VGLUT1 innervation was significantly higher in the deafferented red nucleus of the *Sox9* KO mice six weeks after MCAO, this may have translated into improved function due to enhanced rubrospinal activity. The rubrospinal tract is VGLUT2 positive, which was not analyzed at the deafferented cervical spinal cord in the present study (Liang, Paxinos et al. 2012; Liang, Paxinos et al. 2012). It is also necessary to note that evidence of structural plasticity with tract tracing does not necessarily mean that functional synapses were formed; VGLUT proteins may not have been present in the axon terminals of the BDA-labeled fibers to create functional synapses. Therefore, one explanation for these data is that increased functional connectivity of the contralesional corticospinal tract to the deafferented cervical spinal cord may not have occurred to play a role in the improved functional recovery exhibited by the knockout mice.

On the other hand, Since VGLUT expression at the cervical spinal cord ventral horn was measured over a much larger area than it was at the red nucleus, a difference between genotypes may not have been large enough to be detected and to achieve statistical significance. Perhaps a difference in VGLUT1 staining due to 2.957 ± 0.5663 percent of overall labeled contralesional fibers present at the deafferented cervical spinal cord in the control mice versus 5.856 ± 0.7764 percent in the *Sox9* KO mice was not substantial enough to display a significant difference between genotypes (when immunoreactivity of all sources of VGLUT1 on all neurons of the cervical spinal cord ventral horn was measured). Arguably, a more accurate way to examine possible synapses of interest is to count puncta of synaptic markers around specific cells of interest (e.g. motor neurons in the spinal cord and rubrospinal neurons in the red nucleus). Interestingly enough, recent work done by our research group has shown that numbers of VGLUT1 puncta surrounding motor neurons of the deafferented cervical

spinal cord ventral horn are significantly higher in the *Sox9* KO animals compared to those in the controls after stroke. Thus, it is possible that this difference was simply diluted by the large area that VGLUT1 immunoreactivity was measured over the deafferented cervical spinal cord ventral horn in the present study. Immunohistological co-localization of VGLUT1 and BDA would be another beneficial follow-up experiment to further establish evidence of putative synapses of the contralesional corticospinal tract. VGLUT1 and PSD-95 co-localization would also give insight as to whether or not both pre-and post-synaptic proteins were aligning for proper synapse functionality. Again, electrophysiological studies would be ideal to elucidate these findings.

4.3 Conclusions

Overall, *Sox9* KO animals exhibited improved functional recovery after a 30 minute MCAO compared to control animals. We hypothesized that this may occur due to increased neuroplasticity in the *Sox9* KO animals, since previous studies by our research group showed that *Sox9* ablation caused a decrease in the expression of axon growth-inhibiting CSPGs in the CNS. Tract-tracing findings supported our hypothesis: the *Sox9*-ablated mice exhibited increased contralesional corticofugal structural neuroplasticity compared to control mice when BDA-labeled fibers were analyzed at the denervated red nucleus and cervical spinal cord after MCAO.

Putative synaptic neuroplasticity was examined with markers for presynaptic glutamatergic input within the deafferented areas. *Sox9* KO animals exhibited significantly higher levels of VGLUT1 at the deafferented red nucleus by six weeks after MCAO compared to control mice. Since VGLUT1 is the main VGLUT isoform of the corticorubral tract, this data correlated nicely with the tract tracing findings to support the hypothesis. Higher levels of synaptic neuroplasticity in the *Sox9* KO animals for the thalamorubral, cerebellorubral, or corticospinal tracts (which are also important for motor function) were not evident with the presented immunohistological analyses. Further studies (e.g. counting puncta or co-localizing synaptic markers on cells of interest, as well

as electrophysiological experiments) would be very beneficial to explore neuroplasticity further.

The improved functional recovery observed in the *Sox9* KO mice is certainly interesting. Evidence of increased contralesional corticorubral and corticospinal plasticity is encouraging, and correlates nicely with the previously observed lower levels of CSPGs and PNNs in the *Sox9* KO mice central nervous system. Further unraveling the exact mechanisms that elicited the improved functional recovery observed in *Sox9*-ablated mice after stroke could lead to the development of novel stroke treatments for humans.

References

- . "Allen Brain Atlas - VGlut2 gene in mouse brain." from <http://mouse.brain-map.org/experiment/show/73818754>.
- . "Allen Brain Atlas - VGlut1 gene in mouse brain." from <http://mouse.brain-map.org/experiment/show/70436317>.
- Akiyama, H., M. C. Chaboissier, et al. (2002). "The transcription factor Sox9 has essential roles in successive steps of the chondrocyte differentiation pathway and is required for expression of Sox5 and Sox6." *Genes Dev* **16**(21): 2813-2828.
- Apostolova, I., A. Irintchev, et al. (2006). "Tenascin-R restricts posttraumatic remodeling of motoneuron innervation and functional recovery after spinal cord injury in adult mice." *J Neurosci* **26**(30): 7849-7859.
- Armstead WM, G. K., Kiessling JW, Riley J, Chen XH, Smith DH, Stein SC, Higazi AA, Cines DB, Bdeir K, Zaitsev S, Muzykantov VR (2010). "Signaling, delivery and age as emerging issues in the benefit/risk ratio outcome of tPA For treatment of CNS ischemic disorders." *Journal of Neurochemistry* **113**(2): 303-312.
- Arnault, P., A. Ebrahimi-Gaillard, et al. (1994). "Electron microscopic demonstration of terminations of posterior thalamic axons on identified rubrospinal neurons in the rat." *Anat Embryol (Berl)* **189**(5): 383-392.
- Arvidsson, A., T. Collin, et al. (2002). "Neuronal replacement from endogenous precursors in the adult brain after stroke." *Nat Med* **8**(9): 963-970.
- Barroso-Chinea, P., M. Castle, et al. (2007). "Expression of the mRNAs encoding for the vesicular glutamate transporters 1 and 2 in the rat thalamus." *J Comp Neurol* **501**(5): 703-715.
- Bi, W., W. Huang, et al. (2001). "Haploinsufficiency of Sox9 results in defective cartilage primordia and premature skeletal mineralization." *Proc Natl Acad Sci U S A* **98**(12): 6698-6703.
- Bonita, R. and R. Beaglehole (1988). "Recovery of motor function after stroke." *Stroke* **19**(12): 1497-1500.
- Bradbury, E. J., L. D. Moon, et al. (2002). "Chondroitinase ABC promotes functional recovery after spinal cord injury." *Nature* **416**(6881): 636-640.
- Bregman, B. S., E. Kunkel-Bagden, et al. (1995). "Recovery from spinal cord injury mediated by antibodies to neurite growth inhibitors." *Nature* **378**(6556): 498-501.

- Bromberg, M. B., J. B. Penney, Jr., et al. (1981). "Evidence for glutamate as the neurotransmitter of corticothalamic and corticorubral pathways." Brain Res **215**(1-2): 369-374.
- Brosamle, C., A. B. Huber, et al. (2000). "Regeneration of lesioned corticospinal tract fibers in the adult rat induced by a recombinant, humanized IN-1 antibody fragment." J Neurosci **20**(21): 8061-8068.
- Bruneau, E. G., J. A. Esteban, et al. (2009). "Receptor-associated proteins and synaptic plasticity." FASEB J **23**(3): 679-688.
- Carmichael, S. T. (2003). "Plasticity of cortical projections after stroke." Neuroscientist **9**(1): 64-75.
- Carmichael, S. T. (2005). "Rodent models of focal stroke: size, mechanism, and purpose." NeuroRx **2**(3): 396-409.
- Carmichael, S. T., I. Archibeque, et al. (2005). "Growth-associated gene expression after stroke: evidence for a growth-promoting region in peri-infarct cortex." Experimental neurology **193**(2): 291-311.
- Carulli, D., T. Pizzorusso, et al. (2010). "Animals lacking link protein have attenuated perineuronal nets and persistent plasticity." Brain **133**(Pt 8): 2331-2347.
- Caterson, B., J. E. Christner, et al. (1985). "Production and characterization of monoclonal antibodies directed against connective tissue proteoglycans." Fed Proc **44**(2): 386-393.
- Chen, J., Y. Li, et al. (2001). "Therapeutic benefit of intravenous administration of bone marrow stromal cells after cerebral ischemia in rats." Stroke **32**(4): 1005-1011.
- Cho, K. S., L. Yang, et al. (2005). "Re-establishing the regenerative potential of central nervous system axons in postnatal mice." J Cell Sci **118**(Pt 5): 863-872.
- Chopp, M., Z. G. Zhang, et al. (2007). "Neurogenesis, angiogenesis, and MRI indices of functional recovery from stroke." Stroke **38**(2 Suppl): 827-831.
- Clarke, P., V. Marshall, et al. (2002). "Well-being after stroke in Canadian seniors: findings from the Canadian Study of Health and Aging." Stroke **33**(4): 1016-1021.
- CSN (2011). "The Quality of Stroke Care in Canada."
- CSN. (2012). "Stroke 101." from <http://www.canadianstrokenetwork.ca/index.php/about/about-stroke/stroke-101/>.
- Davies, S. J., M. T. Fitch, et al. (1997). "Regeneration of adult axons in white matter tracts of the central nervous system." Nature **390**(6661): 680-683.

- Dijkhuizen, R. M., A. B. Singhal, et al. (2003). "Correlation between brain reorganization, ischemic damage, and neurologic status after transient focal cerebral ischemia in rats: a functional magnetic resonance imaging study." J Neurosci **23**(2): 510-517.
- Durukan, A. and T. Tatlisumak (2007). "Acute ischemic stroke: overview of major experimental rodent models, pathophysiology, and therapy of focal cerebral ischemia." Pharmacol Biochem Behav **87**(1): 179-197.
- Eddleston, M. and L. Mucke (1993). "Molecular profile of reactive astrocytes-- implications for their role in neurologic disease." Neuroscience **54**(1): 15-36.
- Fawcett, J. W. and R. A. Asher (1999). "The glial scar and central nervous system repair." Brain Res Bull **49**(6): 377-391.
- Feydy, A., R. Carlier, et al. (2002). "Longitudinal study of motor recovery after stroke: recruitment and focusing of brain activation." Stroke **33**(6): 1610-1617.
- Fidler, P. S., K. Schuette, et al. (1999). "Comparing astrocytic cell lines that are inhibitory or permissive for axon growth: the major axon-inhibitory proteoglycan is NG2." J Neurosci **19**(20): 8778-8788.
- Fink, A. J., C. Englund, et al. (2006). "Development of the deep cerebellar nuclei: transcription factors and cell migration from the rhombic lip." J Neurosci **26**(11): 3066-3076.
- Fujii, Y. and T. Nakada (2003). "Cortical reorganization in patients with subcortical hemiparesis: neural mechanisms of functional recovery and prognostic implication." J Neurosurg **98**(1): 64-73.
- Fukuta, M., K. Uchimura, et al. (1995). "Molecular cloning and expression of chick chondrocyte chondroitin 6-sulfotransferase." J Biol Chem **270**(31): 18575-18580.
- Gallo, V. and A. Bertolotto (1990). "Extracellular matrix of cultured glial cells: selective expression of chondroitin 4-sulfate by type-2 astrocytes and their progenitors." Exp Cell Res **187**(2): 211-223.
- Galtrey, C. M. and J. W. Fawcett (2007). "The role of chondroitin sulfate proteoglycans in regeneration and plasticity in the central nervous system." Brain Res Rev **54**(1): 1-18.
- Gorelick, P. B. and S. Ruland (2010). "Update of cerebral vascular disease: issues for the primary care physician." Dis Mon **56**(2): 40-71.
- Gotting, C., J. Kuhn, et al. (2000). "Molecular cloning and expression of human UDP-d-Xylose:proteoglycan core protein beta-d-xylosyltransferase and its first isoform XT-II." J Mol Biol **304**(4): 517-528.

- GrandPre, T., S. Li, et al. (2002). "Nogo-66 receptor antagonist peptide promotes axonal regeneration." Nature **417**(6888): 547-551.
- Grigoryan, M. and A. I. Qureshi (2010). "Acute stroke management: endovascular options for treatment." Semin Neurol **30**(5): 469-476.
- Grimpe, B. and J. Silver (2004). "A novel DNA enzyme reduces glycosaminoglycan chains in the glial scar and allows microtransplanted dorsal root ganglia axons to regenerate beyond lesions in the spinal cord." J Neurosci **24**(6): 1393-1397.
- Gris, P., A. Tighe, et al. (2007). "Transcriptional regulation of scar gene expression in primary astrocytes." Glia **55**(11): 1145-1155.
- Herz, J., R. Reitmeir, et al. (2012). "Intracerebroventricularly delivered VEGF promotes contralesional corticorubral plasticity after focal cerebral ischemia via mechanisms involving anti-inflammatory actions." Neurobiol Dis **45**(3): 1077-1085.
- Huang, D. W., L. McKerracher, et al. (1999). "A therapeutic vaccine approach to stimulate axon regeneration in the adult mammalian spinal cord." Neuron **24**(3): 639-647.
- Jiang, M. C., G. F. Alheid, et al. (2002). "Cerebellar input to magnocellular neurons in the red nucleus of the mouse: synaptic analysis in horizontal brain slices incorporating cerebello-rubral pathways." Neuroscience **110**(1): 105-121.
- Johansson, B. B. (2000). "Brain plasticity and stroke rehabilitation. The Willis lecture." Stroke **31**(1): 223-230.
- Katsman, D., J. Zheng, et al. (2003). "Tissue microenvironments within functional cortical subdivisions adjacent to focal stroke." J Cereb Blood Flow Metab **23**(9): 997-1009.
- Kearns, A. E., S. C. Campbell, et al. (1991). "Initiation of chondroitin sulfate biosynthesis: a kinetic analysis of UDP-D-xylose: core protein beta-D-xylosyltransferase." Biochemistry **30**(30): 7477-7483.
- Kilic, E., A. ElAli, et al. (2010). "Role of Nogo-A in neuronal survival in the reperfused ischemic brain." J Cereb Blood Flow Metab **30**(5): 969-984.
- Lansberg, M. G., E. Bluhmki, et al. (2009). "Efficacy and safety of tissue plasminogen activator 3 to 4.5 hours after acute ischemic stroke: a metaanalysis." Stroke **40**(7): 2438-2441.
- Lee, J. K., J. E. Kim, et al. (2004). "Nogo receptor antagonism promotes stroke recovery by enhancing axonal plasticity." The Journal of neuroscience : the official journal of the Society for Neuroscience **24**(27): 6209-6217.

- Lee, J. M., M. C. Grabb, et al. (2000). "Brain tissue responses to ischemia." J Clin Invest **106**(6): 723-731.
- Lemon, R. N. (2008). "Descending pathways in motor control." Annu Rev Neurosci **31**: 195-218.
- Lemons, M. L., J. D. Sandy, et al. (2003). "Intact aggrecan and chondroitin sulfate-depleted aggrecan core glycoprotein inhibit axon growth in the adult rat spinal cord." Exp Neurol **184**(2): 981-990.
- Li, H. P., A. Homma, et al. (2007). "Regeneration of nigrostriatal dopaminergic axons by degradation of chondroitin sulfate is accompanied by elimination of the fibrotic scar and glia limitans in the lesion site." J Neurosci Res **85**(3): 536-547.
- Li, S. and S. M. Strittmatter (2003). "Delayed systemic Nogo-66 receptor antagonist promotes recovery from spinal cord injury." J Neurosci **23**(10): 4219-4227.
- Li, X., K. K. Blizzard, et al. (2004). "Chronic behavioral testing after focal ischemia in the mouse: functional recovery and the effects of gender." Exp Neurol **187**(1): 94-104.
- Liang, H., G. Paxinos, et al. "The red nucleus and the rubrospinal projection in the mouse." Brain Structure and Function **217**(2): 221-232.
- Liang, H., G. Paxinos, et al. (2012). "The red nucleus and the rubrospinal projection in the mouse." Brain structure & function **217**(2): 221-232.
- Liu, F. and L. D. McCullough (2011). "Middle cerebral artery occlusion model in rodents: methods and potential pitfalls." J Biomed Biotechnol **2011**: 464701.
- Lu, L. (2011). "Evaluation and Management of Ischemic Stroke." McMaster University Medical J **8**(1): 39-44.
- McKeon, R. J., R. C. Schreiber, et al. (1991). "Reduction of neurite outgrowth in a model of glial scarring following CNS injury is correlated with the expression of inhibitory molecules on reactive astrocytes." J Neurosci **11**(11): 3398-3411.
- McKillop, W. M., M. Dragan, et al. (2013). "Conditional Sox9 ablation reduces chondroitin sulfate proteoglycan levels and improves motor function following spinal cord injury." Glia **61**(2): 164-177.
- Meiners, S., E. M. Powell, et al. (1995). "A distinct subset of tenascin/CS-6-PG-rich astrocytes restricts neuronal growth in vitro." J Neurosci **15**(12): 8096-8108.
- Moechars, D., M. C. Weston, et al. (2006). "Vesicular glutamate transporter VGLUT2 expression levels control quantal size and neuropathic pain." J Neurosci **26**(46): 12055-12066.

- Moniot, B., F. Declosmenil, et al. (2009). "The PGD2 pathway, independently of FGF9, amplifies SOX9 activity in Sertoli cells during male sexual differentiation." Development **136**(11): 1813-1821.
- Moser, D. K., L. P. Kimble, et al. (2006). "Reducing delay in seeking treatment by patients with acute coronary syndrome and stroke: a scientific statement from the American Heart Association Council on cardiovascular nursing and stroke council." Circulation **114**(2): 168-182.
- Moskowitz, M. A., E. H. Lo, et al. (2010). "The science of stroke: mechanisms in search of treatments." Neuron **67**(2): 181-198.
- Muir, G. D. and I. Q. Whishaw (2000). "Red nucleus lesions impair overground locomotion in rats: a kinetic analysis." Eur J Neurosci **12**(3): 1113-1122.
- Murphy, T. H. and D. Corbett (2009). "Plasticity during stroke recovery: from synapse to behaviour." Nat Rev Neurosci **10**(12): 861-872.
- Naus, C. C., B. A. Flumerfelt, et al. (1986). "Contralateral corticorubral fibers induced by neonatal lesions are not collaterals of the normal ipsilateral projection." Neurosci Lett **70**(1): 52-58.
- NINDS (1995). "Tissue Plasminogen Activator for Acute Ischemic Stroke. The National Institute of Neurological Disorders and Stroke rt-PA Stroke Study Group." New England Journal of Medicine **333**: 1581-1588.
- O'Neill, M. J. and J. A. Clemens (2001). "Rodent models of focal cerebral ischemia." Curr Protoc Neurosci **Chapter 9**: Unit9 6.
- Papadopoulos, C. M., S. Y. Tsai, et al. (2002). "Functional recovery and neuroanatomical plasticity following middle cerebral artery occlusion and IN-1 antibody treatment in the adult rat." Ann Neurol **51**(4): 433-441.
- Parent, J. M., Z. S. Vexler, et al. (2002). "Rat forebrain neurogenesis and striatal neuron replacement after focal stroke." Ann Neurol **52**(6): 802-813.
- PHAC. (2009). "Tracking Heart Disease and Stroke in Canada." from <http://www.phac-aspc.gc.ca/publicat/2009/cvd-avc/pdf/cvd-avs-2009-eng.pdf>.
- PHAC. (2011). "Tracking Heart Disease and Stroke in Canada - Stroke Highlights." from http://www.phac-aspc.gc.ca/cd-mc/cvd-mcv/sh-fs-2011/pdf/StrokeHighlights_EN.pdf.
- Pineiro, R., S. Pendlebury, et al. (2001). "Functional MRI detects posterior shifts in primary sensorimotor cortex activation after stroke: evidence of local adaptive reorganization?" Stroke **32**(5): 1134-1139.

- Popp, A., N. Jaenisch, et al. (2009). "Identification of ischemic regions in a rat model of stroke." PLoS One **4**(3): e4764.
- Reding, M. J. and E. Potes (1988). "Rehabilitation outcome following initial unilateral hemispheric stroke. Life table analysis approach." Stroke **19**(11): 1354-1358.
- Reitmeir, R., E. Kilic, et al. (2011). "Post-acute delivery of erythropoietin induces stroke recovery by promoting perilesional tissue remodelling and contralesional pyramidal tract plasticity." Brain **134**(Pt 1): 84-99.
- Roger, M. and J. Cadusseau (1987). "Anatomical evidence of a reciprocal connection between the posterior thalamic nucleus and the parvocellular division of the red nucleus in the rat. A combined retrograde and anterograde study." Neuroscience **21**(2): 573-583.
- Rouiller, E. M., F. Liang, et al. (1991). "Trajectory of redirected corticospinal axons after unilateral lesion of the sensorimotor cortex in neonatal rat; A phaseolus vulgaris-leucoagglutinin (PHA-L) tracing study." Experimental Neurology **114**(1): 53-65.
- Rouiller, E. M., F. Y. Liang, et al. (1991). "Trajectory of redirected corticospinal axons after unilateral lesion of the sensorimotor cortex in neonatal rat; a phaseolus vulgaris-leucoagglutinin (PHA-L) tracing study." Exp Neurol **114**(1): 53-65.
- Rovira, A., E. Grive, et al. (2005). "Distribution territories and causative mechanisms of ischemic stroke." Eur Radiol **15**(3): 416-426.
- Rupadevi, M., S. Parasuraman, et al. (2011). "Protocol for middle cerebral artery occlusion by an intraluminal suture method." J Pharmacol Pharmacother **2**(1): 36-39.
- Sacco, R. L., E. J. Benjamin, et al. (1997). "American Heart Association Prevention Conference. IV. Prevention and Rehabilitation of Stroke. Risk factors." Stroke **28**(7): 1507-1517.
- Schaechter, J. D., E. Kraft, et al. (2002). "Motor recovery and cortical reorganization after constraint-induced movement therapy in stroke patients: a preliminary study." Neurorehabil Neural Repair **16**(4): 326-338.
- Schallert, T., S. M. Fleming, et al. (2000). "CNS plasticity and assessment of forelimb sensorimotor outcome in unilateral rat models of stroke, cortical ablation, parkinsonism and spinal cord injury." Neuropharmacology **39**(5): 777-787.
- Schmalfeldt, M., C. E. Bandtlow, et al. (2000). "Brain derived versican V2 is a potent inhibitor of axonal growth." J Cell Sci **113** (Pt 5): 807-816.
- Schnell, L. and M. E. Schwab (1990). "Axonal regeneration in the rat spinal cord produced by an antibody against myelin-associated neurite growth inhibitors." Nature **343**(6255): 269-272.

- Schwartz, N. B. (1977). "Regulation of chondroitin sulfate synthesis. Effect of beta-xylosides on synthesis of chondroitin sulfate proteoglycan, chondroitin sulfate chains, and core protein." J Biol Chem **252**(18): 6316-6321.
- Semkova, I. and J. Krieglstein (1999). "Neuroprotection mediated via neurotrophic factors and induction of neurotrophic factors." Brain Res Brain Res Rev **30**(2): 176-188.
- Siegel, A., and Sapru, H.N. (2010). *Essential Neuroscience*, Lippincott Williams & Wilkins.
- Silver, J. and J. H. Miller (2004). "Regeneration beyond the glial scar." Nat Rev Neurosci **5**(2): 146-156.
- Small, S. L., P. Hlustik, et al. (2002). "Cerebellar hemispheric activation ipsilateral to the paretic hand correlates with functional recovery after stroke." Brain **125**(Pt 7): 1544-1557.
- Snappyan, M., M. Lemasson, et al. (2009). "Vasculature guides migrating neuronal precursors in the adult mammalian forebrain via brain-derived neurotrophic factor signaling." J Neurosci **29**(13): 4172-4188.
- Soleman, S., P. K. Yip, et al. (2012). "Delayed treatment with chondroitinase ABC promotes sensorimotor recovery and plasticity after stroke in aged rats." Brain **135**(Pt 4): 1210-1223.
- StatsCan. (2012). "Leading causes of death, by sex (both sexes)." from <http://www.statcan.gc.ca/tables-tableaux/sum-som/l01/cst01/hlth36a-eng.htm>.
- Varoqui, H., M. K. Schafer, et al. (2002). "Identification of the differentiation-associated Na⁺/PI transporter as a novel vesicular glutamate transporter expressed in a distinct set of glutamatergic synapses." J Neurosci **22**(1): 142-155.
- Veerbeek, J. M., E. van Wegen, et al. (2014). "What is the evidence for physical therapy poststroke? A systematic review and meta-analysis." PLoS One **9**(2): e87987.
- Wade, D. T. and R. L. Hower (1987). "Functional abilities after stroke: measurement, natural history and prognosis." J Neurol Neurosurg Psychiatry **50**(2): 177-182.
- Wang, D. and J. Fawcett (2012). "The perineuronal net and the control of CNS plasticity." Cell Tissue Res **349**(1): 147-160.
- WHO. (2013). "The 10 leading causes of death in the world, 2000 and 2011." from <http://www.who.int/mediacentre/factsheets/fs310/en/>.
- Wilson, N. R., J. Kang, et al. (2005). "Presynaptic regulation of quantal size by the vesicular glutamate transporter VGLUT1." J Neurosci **25**(26): 6221-6234.

- Yamauchi, S., S. Mita, et al. (2000). "Molecular cloning and expression of chondroitin 4-sulfotransferase." J Biol Chem **275**(12): 8975-8981.
- Z'Graggen, W. J., G. A. Metz, et al. (1998). "Functional recovery and enhanced corticofugal plasticity after unilateral pyramidal tract lesion and blockade of myelin-associated neurite growth inhibitors in adult rats." J Neurosci **18**(12): 4744-4757.
- Zai, L., C. Ferrari, et al. (2009). "Inosine alters gene expression and axonal projections in neurons contralateral to a cortical infarct and improves skilled use of the impaired limb." J Neurosci **29**(25): 8187-8197.
- Zemke, A. C., P. J. Heagerty, et al. (2003). "Motor cortex organization after stroke is related to side of stroke and level of recovery." Stroke **34**(5): e23-28.
- Zhang, L., T. Schallert, et al. (2002). "A test for detecting long-term sensorimotor dysfunction in the mouse after focal cerebral ischemia." J Neurosci Methods **117**(2): 207-214.
- Zhao, S., M. Zhao, et al. (2013). "Constraint-induced movement therapy overcomes the intrinsic axonal growth-inhibitory signals in stroke rats." Stroke **44**(6): 1698-1705.
- Zorowitz R, B. E., Cuccurullo S. (2004). Types of Stroke. Physical Medicine and Rehabilitation Board Review. C. S. New York Demos Medical Publishing.
- Zuo, J., D. Neubauer, et al. (1998). "Degradation of chondroitin sulfate proteoglycan enhances the neurite-promoting potential of spinal cord tissue." Exp Neurol **154**(2): 654-662.



007-009-02::6:

AUP Number: 2007-009-02

AUP Title: Molecular and Cellular Studies of Spinal Cord Injury in Mice and Rats

Yearly Renewal Date: 06/01/2013

The YEARLY RENEWAL to Animal Use Protocol (AUP) 2007-009-02 has been approved, and will be approved for one year following the above review date.

1. This AUP number must be indicated when ordering animals for this project.
2. Animals for other projects may not be ordered under this AUP number.
3. Purchases of animals other than through this system must be cleared through the ACVS office.
Health certificates will be required.

REQUIREMENTS/COMMENTS

Please ensure that the individual(s) performing procedures on live animals, as described in this protocol, are familiar with the contents of this document.

The holder of this Animal Use Protocol is responsible to ensure that all associated safety components (biosafety, radiation safety, general laboratory safety) comply with institutional safety standards and have received all necessary approvals. Please consult directly with your institutional safety officers.

Submitted by: Mollard, Maureen
on behalf of the Animal Use Subcommittee

Curriculum Vitae

Name: Bethany Bass

Post-secondary Education and Degrees: Western University
London, Ontario, Canada
B. MSc. Medical Sciences and Anatomy and Cell Biology (Honors)
2006-2010

Western University
London, Ontario, Canada
M. Sc. Anatomy and Cell Biology
2011-2014

Honours and Awards: Western Graduate Research Scholarship
2011-2013

CIHR Strategic Training Program in Vascular Research
2011-2013

Province of Ontario Graduate Scholarship
2012-2013

Related Work Experience: Teaching Assistant
Mammalian Histology, ACB 3309
The University of Western Ontario
2011-2013

Poster Presentations: Bass, B. *Sox9* ablation improves recovery in a mouse model of ischemic stroke. Anatomy and Cell Biology Research Day. Western University. 2013.

Bass, B. Sox9 ablation improves recovery in a mouse model of ischemic stroke. London Health Research Day. 2013.